



**Extraterrestrial Prebiotic Molecules: Photochemistry vs.  
Radiation Chemistry of  
Interstellar Ices**

Journal:	<i>Chemical Society Reviews</i>
Manuscript ID	CS-SYN-06-2017-000443.R2
Article Type:	Tutorial Review
Date Submitted by the Author:	06-Jan-2019
Complete List of Authors:	Arumainayagam, Christopher; Wellesley College, Chemistry Garrod, Robin; University of Virginia, Chemistry Boyer, Michael; Clark University, Physics Hay, Aurland; Wellesley College, Chemistry Bao, Si Tong; Wellesley College, Chemistry Campbell, Jyoti; Wellesley College, Chemistry Wang, Amy; Wellesley College, Chemistry Nowak, Christopher; Wellesley College, Chemistry Arumainayagam, Michael; Wellesley College, Chemistry Hodge, Peter; Wellesley College, Chemistry

## **Extraterrestrial Prebiotic Molecules: Photochemistry vs. Radiation Chemistry of Interstellar Ices**

Chris R. Arumainayagam, Robin T. Garrod, Michael Boyer, Aurland Hay, Si Tong Bao, Jyoti Campbell, Amy Wang, Chris M. Nowak, Michael R. Arumainayagam, and Peter J. Hodge

In 2016, unambiguous evidence for the presence of the amino acid glycine, an important prebiotic molecule, was deduced based on in situ mass-spectral studies of the coma surrounding cometary ice. This finding is significant because comets are thought to have preserved the icy grains originally found in the interstellar medium prior to solar system formation. Energetic processing of cosmic ices via photochemistry and radiation chemistry is thought to be the dominant mechanism for the extraterrestrial synthesis of prebiotic molecules. Radiation chemistry is defined as the “study of the chemical changes produced by the absorption of radiation of sufficiently high energy to produce ionization.” Ionizing radiation in cosmic chemistry includes high-energy particles (e.g., cosmic rays) and high-energy photons (e.g., extreme-UV). In contrast, photochemistry is defined as chemical processes initiated by photon-induced electronic excitation not involving ionization. Vacuum-UV (6.2–12.4 eV) light may, in addition to photochemistry, initiate radiation chemistry because the threshold for producing secondary electrons is lower in the condensed phase than in the gas phase. Unique to radiation chemistry are four phenomena: (1) production of a cascade of low-energy (< 20 eV) secondary electrons which are thought to be the dominant driving force for radiation chemistry, (2) reactions initiated by cations, (3) non-uniform distribution of reaction intermediates, and (4) non-selective chemistry leading to the production of multiple reaction products. The production of low-energy secondary electrons during radiation chemistry may also lead to new reaction pathways not available to photochemistry. In addition, low-energy electron-induced radiation chemistry may predominate over photochemistry because of the sheer number of low-energy secondary electrons. Moreover, reaction cross-sections can be several orders of magnitude larger for electrons than for photons. Discerning the role of photochemistry vs. radiation chemistry in astrochemistry is challenging because astrophysical photon-induced chemistry studies have almost exclusively used light sources that produce > 10 eV photons. Because a primary objective of chemistry is to provide molecular-level mechanistic explanations for macroscopic phenomena, our ultimate goal in this review paper is to critically evaluate our current understanding of cosmic ice energetic processing which likely leads to the synthesis of extraterrestrial prebiotic molecules.

## Extraterrestrial Prebiotic Molecules: Photochemistry vs. Radiation Chemistry of Interstellar Ices

### 1. Introduction:

According to a recently published book, *The Stardust Revolution*, we are in the midst of the third scientific revolution, after those of Copernicus and Darwin.<sup>1</sup> This book espouses the view that the origin of life can be traced back to the stars themselves. Indeed, during the past several decades, complex organic molecules (COMs)<sup>a</sup> have been routinely detected toward star-forming cores (of size < 0.2 light-years), commonly known as “hot cores” or “hot molecular cores,” within which the precursors of hot, high-mass<sup>b</sup> stars are gradually forming.<sup>2</sup> More recently, measurements from the revolutionary Atacama Large Millimeter/submillimeter Array (ALMA) telescope have uncovered a comparable degree of chemical complexity in the dusty envelopes of smaller, sun-like protostars, known as “hot corinos”—the low-mass analogs of hot molecular cores. The first detections of molecules (CH in 1937 and CN in 1940) in space were initially surprising because of “inhospitable” conditions such as: (1) low temperatures (10 – 100 K) that are usually thought to inhibit chemical synthesis, (2) near zero pressures ( $10^{-14}$  atmospheres) that reduce reaction rates by lowering the molecular collision frequency, and (3) intense ionizing radiation (now known to include cosmic rays with energies as high as  $10^{21}$  eV) that is capable of destroying molecules. Not surprisingly, in 1926 during a Royal Society lecture, Sir Arthur Eddington claimed that no known mechanism could account for the significant presence of extraterrestrial molecules.

Many viable gas-phase mechanisms exist for the production of simple molecules such as CO, and even for simple hydrides like water and ammonia. However, while some current studies suggest a gas-phase interstellar formation mechanism for larger molecules such as formamide ( $\text{HCONH}_2$ ),<sup>3</sup> a potential precursor for both genetic and metabolic molecules, the currently accepted view is that energetic ice processing is the main mechanism responsible for the interstellar synthesis of most saturated organic molecules considered to be prebiotic molecules.<sup>c</sup> In this review, we explore the different underlying interstellar condensed-phase chemical synthesis mechanisms, with emphasis on the fundamentals of photochemistry and radiation chemistry of ices in star-

---

<sup>a</sup> In the field of astrochemistry, molecules containing six or more atoms are commonly called complex organic molecules. A recent development is the term iCOM where i denotes interstellar.

<sup>b</sup> High mass stars are typically defined as stars whose mass exceeds eight times the mass of the sun.

<sup>c</sup> Atom addition (e.g., sequential hydrogenation of CO to form  $\text{CH}_3\text{OH}$ ) is one example of a “non-energetic processing” mechanism for the chemical transformation of interstellar ices.

2 atoms	CS	HCO <sup>+</sup>	KCN	H <sub>3</sub> O <sup>+</sup>	HCOOH	<i>l</i> -HC <sub>3</sub> N	CH <sub>2</sub> CHCHO	CH <sub>3</sub> OCH <sub>2</sub> OH
H <sub>2</sub>	HF	HCS <sup>+</sup>	FeCN	NH <sub>3</sub>	H <sub>2</sub> CNH	<i>c</i> -H <sub>2</sub> C <sub>3</sub> O	CH <sub>2</sub> CCHCN	11 atoms
AlF	SH	HOC <sup>+</sup>	HO <sub>2</sub>	<i>c</i> -SiC <sub>3</sub>	H <sub>2</sub> C <sub>2</sub> O	C <sub>5</sub> N <sup>-</sup>	H <sub>2</sub> NCH <sub>2</sub> CN	HC <sub>9</sub> N
AlCl	SH <sup>+</sup>	H <sub>2</sub> O	TiO <sub>2</sub>	CH <sub>3</sub>	H <sub>2</sub> NCN	E-HNCHCN	CH <sub>3</sub> CHNH	CH <sub>3</sub> C <sub>6</sub> H
C <sub>2</sub>	FeO	H <sub>2</sub> S	C <sub>2</sub> N	C <sub>3</sub> N <sup>-</sup>	HNC <sub>3</sub>	SiH <sub>3</sub> CN	CH <sub>3</sub> SiH <sub>3</sub>	C <sub>2</sub> H <sub>5</sub> OCHO
CH	O <sub>2</sub>	HNC	SiCSi	PH <sub>3</sub>	SiH <sub>4</sub>	CH <sub>2</sub> CNH	C <sub>2</sub> H <sub>5</sub> N	CH <sub>3</sub> OC(O)CH <sub>3</sub>
CH <sup>+</sup>	CF <sup>+</sup>	HNO	S <sub>2</sub> H	HCNO	H <sub>2</sub> COH <sup>+</sup>	C <sub>5</sub> S	(NH <sub>2</sub> ) <sub>2</sub> CO	12 atoms
CN	PO	MgCN	HCS	HOCN	C <sub>4</sub> H <sup>-</sup>	7 atoms	9 atoms	<i>c</i> -C <sub>6</sub> H <sub>6</sub>
CO	AlO	MgNC	HSC	HSCN	HC(O)CN	C <sub>6</sub> H	CH <sub>3</sub> C <sub>4</sub> H	C <sub>3</sub> H <sub>2</sub> CN
CO <sup>+</sup>	CN <sup>-</sup>	N <sub>2</sub> H <sup>+</sup>	NCO	H <sub>2</sub> O <sub>2</sub>	HNCNH	CH <sub>2</sub> CHCN	CH <sub>3</sub> CH <sub>2</sub> CN	<i>t</i> -C <sub>2</sub> H <sub>5</sub> OCH <sub>3</sub>
CP	HCl <sup>+</sup>	N <sub>2</sub> O	OCN <sup>-</sup>	<i>l</i> -C <sub>3</sub> H <sup>+</sup>	CH <sub>3</sub> O	HC <sub>5</sub> N	(CH <sub>3</sub> ) <sub>2</sub> O	>12 atoms
CSi	TiO	NaCN	4 atoms	HMgNC	H <sub>2</sub> NCO <sup>+</sup>	CH <sub>3</sub> CHO	CH <sub>3</sub> CH <sub>2</sub> OH	C <sub>60</sub>
HCl	ArH <sup>+</sup>	OCS	C <sub>3</sub> H <sup>+</sup>	HCCO	NCCNH <sup>+</sup>	NH <sub>2</sub> CH <sub>3</sub>	HC <sub>7</sub> N	C <sub>60</sub> <sup>+</sup>
KCl	N <sub>2</sub>	SO <sub>2</sub>	<i>l</i> -C <sub>3</sub> H <sup>+</sup>	CH <sub>3</sub> Cl	NH <sub>3</sub> D <sup>+</sup>	<i>c</i> -C <sub>2</sub> H <sub>4</sub> O	C <sub>6</sub> H	C <sub>70</sub>
NH	NO <sup>+</sup>	<i>c</i> -SiC <sub>2</sub>	C <sub>3</sub> N	CNCN	6 atoms	H <sub>2</sub> CCHOH	CH <sub>3</sub> C(O)NH <sub>2</sub>	<i>c</i> -C <sub>6</sub> H <sub>5</sub> CN
NO	NS <sup>+</sup>	CO <sub>2</sub>	C <sub>3</sub> O	MgCCH	C <sub>5</sub> H	C <sub>6</sub> H <sup>-</sup>	C <sub>6</sub> H <sup>+</sup>	CO(CH <sub>2</sub> OH) <sub>2</sub> ?
NS	LiH	NH <sub>2</sub>	C <sub>3</sub> S	NCCP	<i>l</i> -C <sub>4</sub> H <sub>2</sub>	CH <sub>3</sub> NCO	C <sub>3</sub> H <sub>6</sub>	C <sub>14</sub> H <sub>10</sub> ?
NaCl	CrO	H <sub>3</sub> <sup>+</sup>	C <sub>2</sub> H <sub>2</sub>	5 atoms	C <sub>2</sub> H <sub>4</sub>	HC <sub>5</sub> O	CH <sub>3</sub> CH <sub>2</sub> SH	C <sub>14</sub> H <sub>10</sub> <sup>+</sup>
OH	3 atoms	SiCN	HC <sub>2</sub> N	C <sub>5</sub>	CH <sub>3</sub> CN	8 atoms	CH <sub>3</sub> NHCHO	C <sub>6</sub> H <sub>5</sub> OH
OH <sup>+</sup>	C <sub>3</sub>	AlNC	HCNH <sup>+</sup>	C <sub>4</sub> H	CH <sub>3</sub> CN	CH <sub>3</sub> C <sub>3</sub> N	HC <sub>7</sub> O	
PN	C <sub>2</sub> H	SiNC	HNCO	C <sub>4</sub> Si	CH <sub>3</sub> OH	HC(O)OCH <sub>3</sub>	10 atoms	
SO	C <sub>2</sub> O	HCP	HNCS	<i>c</i> -C <sub>3</sub> H <sub>2</sub>	CH <sub>3</sub> SH	CH <sub>3</sub> COOH	CH <sub>3</sub> C <sub>3</sub> N	
SO <sup>+</sup>	C <sub>2</sub> S	CCP	HOCO <sup>+</sup>	CH <sub>2</sub> CN	HC <sub>3</sub> NH <sup>+</sup>	C <sub>7</sub> H	(CH <sub>3</sub> ) <sub>2</sub> CO	
SiN	CH <sub>2</sub>	AlOH	H <sub>2</sub> CO	CH <sub>4</sub>	HC <sub>2</sub> CHO	H <sub>2</sub> C <sub>6</sub>	(CH <sub>2</sub> OH) <sub>2</sub>	
SiO	HCN	H <sub>2</sub> O <sup>+</sup>	H <sub>2</sub> CN	HC <sub>3</sub> N	NH <sub>2</sub> CHO	CH <sub>2</sub> OHCHO	CH <sub>3</sub> CH <sub>2</sub> CHO	
SiS	HCO	H <sub>2</sub> Cl <sup>+</sup>	H <sub>2</sub> CS	HC <sub>2</sub> NC	C <sub>3</sub> N	<i>l</i> -C <sub>6</sub> H <sub>2</sub>	CH <sub>3</sub> CHCH <sub>2</sub> O	

\*Both linear and cyclic C<sub>3</sub>H

Table 1

Source: [http://astrochymist.org/astrochymist\\_ism.html](http://astrochymist.org/astrochymist_ism.html) (accessed January 2019)

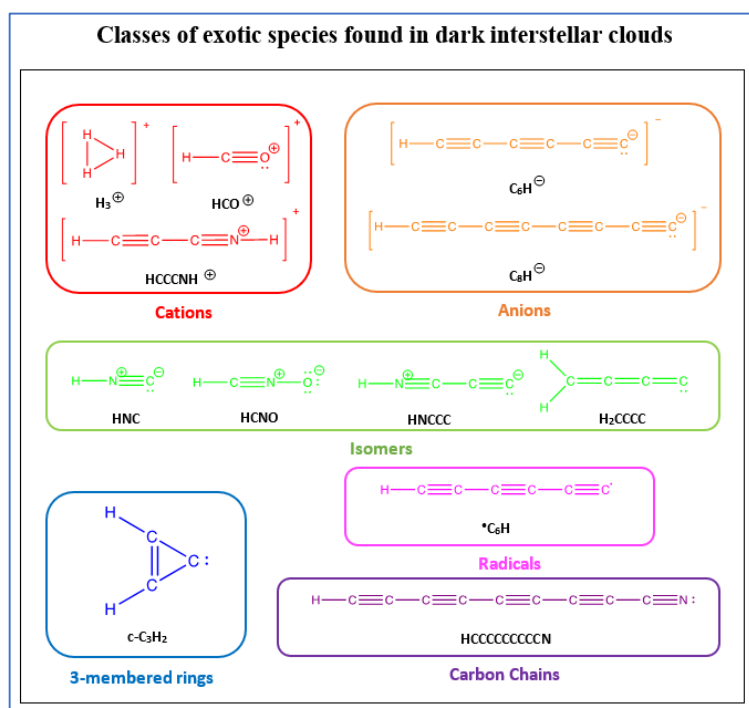


Figure 1

Classes of "exotic species" found in dark clouds. CREDIT: Eric Herbst (University of Virginia)

forming regions. Specifically, we wish to dispel the common misconception in astrochemistry

that UV photons only induce photochemistry and do not initiate radiation chemistry.

## 1.1 Cosmic Chemistry Cycle

Ever since the discovery of the still enigmatic<sup>d</sup> spectral diffuse interstellar bands (DIB) about 100 years ago,<sup>e</sup> we have

suspected that the interstellar medium (ISM), the space between star systems in a galaxy, contains molecules, especially near star-forming regions.<sup>f</sup> In addition to these diffuse interstellar bands which are electronic spectral absorption bands, vibrational emission bands have been used to telescopically identify complex molecules such as polycyclic aromatic hydrocarbons<sup>g</sup> (PAHs), fullerenes (C<sub>60</sub>, C<sub>70</sub>), and diamondoids. Cosmic ices have been characterized by vibrational absorption bands. To date, molecular rotational emission

<sup>d</sup> In 2015, C<sub>60</sub><sup>+</sup> was unambiguously identified as the carrier of two of the diffuse interstellar bands.

<sup>e</sup> The earliest observation of DIB is to be found in a photographic plate likely taken by Annie Jump Cannon who graduated in 1884 from Wellesley College, the school with which a number of authors of this article are associated.

<sup>f</sup> Most of the interstellar medium, however, consists of hot regions (coronal gas, warm ionized, HII, and warm neutral) which are not conducive to the synthesis of molecules.

<sup>g</sup> PAH consist of concatenated aromatic rings.

from cm to submillimeter wavelengths, has been exploited to identify, within interstellar and circumstellar clouds,<sup>h</sup> over 200 different (not counting isotopologues) gas-phase molecules (Table 1), including “exotic” molecules such as cations (e.g.,  $\text{H}_3^+$ ), anions (e.g.,  $\text{C}_6\text{H}^-$ ), less-stable isomers (e.g., HNC),<sup>i</sup> three-membered rings (e.g., cyclopropenylidene, or  $c\text{-C}_3\text{H}_2$ ), radicals (e.g.,  $\bullet\text{C}_6\text{H}$ ), and carbon chains ( $\text{HC}_9\text{N}$ ) (Figure 1). Most notably, Table 1 contains several potential prebiotic molecules such as cyanomethanimine ( $\text{NC}_2\text{H}_2\text{NH}$ ), which is a precursor of adenine, one of the four nucleobases of DNA. Fundamental to understanding how complex and/or prebiotic molecules are synthesized in the interstellar medium is the cosmic chemistry cycle<sup>j</sup> (Figure 2) which consists of five stages: (1) diffuse cloud, (2) dense cloud, (3) protostar with accretion disk, (4) fully formed stellar system, and (5) stellar mass loss, recycling elements back into a diffuse cloud. Figure 2 also illustrates the possibility of prebiotic organic molecules being delivered to planets by meteorites or comets. Recent simulations demonstrate the possibility of amino acid synthesis and survival during impact of cometary ices on Earth.<sup>4</sup>

Diffuse clouds (diffuse interstellar medium), the smallest overdensity in the interstellar medium, have

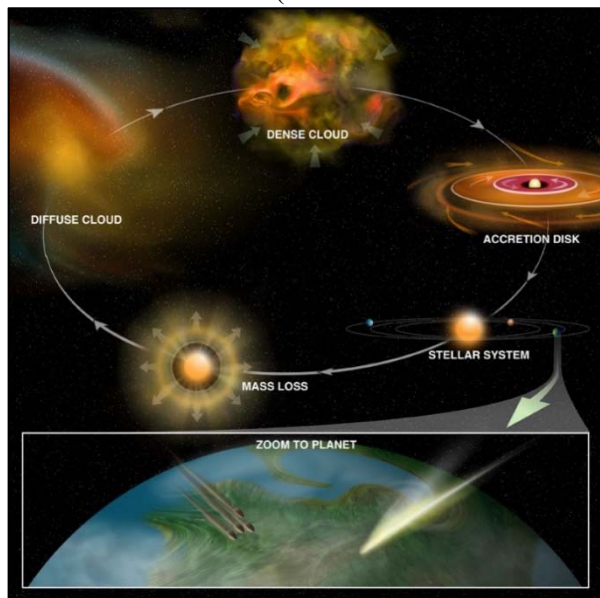


**Figure 2**  
Cosmic Chemistry Cycle  
CREDIT: Bill Saxton, NRAO/AUI/NSF

densities of  $10^2 - 10^3$  atoms/molecules per  $\text{cm}^3$  and gas kinetic temperatures of around 100 K. While permeated by microscopic ( $\sim 0.1 \mu\text{m}$ ) dust grains, the diffuse interstellar medium is relatively transparent to visible light, with an optical depth<sup>k</sup> of  $\leq 1$ . Except for the formation of molecular hydrogen, the universe’s most abundant molecule which forms primarily on dust grain surfaces, the limited chemistry in the diffuse interstellar medium is typically dominated by gas phase reactions, leading to the production of small molecules (including long-lived radicals such as CN). The

<sup>h</sup> To date, over 80 different molecular species have been discovered in circumstellar envelopes which surround evolved stars.

<sup>i</sup> Because of low temperatures most interstellar chemical reactions are under kinetic control which enhances the yield of the less stable product (e.g., HNC) at the expense of the more stable product (e.g., HCN).

<sup>j</sup> The history of the cosmic chemistry cycle can perhaps be traced back to the so called “nebulae hypothesis” attributable to contributions by Emanuel Swedenborg in 1734, Immanuel Kant in 1755, and Pierre-Simon Laplace in 1796.

<sup>k</sup> “Optical depth” or “optical thickness”,  $\tau$ , a measure of transparency, is defined as the negative of the natural logarithm of transmission. Note the similarity between the definitions of optical depth ( $\tau = -\ln T$ ) and absorbance ( $\tau = -\log_{10} T$ ).

magnetic-field influenced gravitational collapse of diffuse clouds forms dark, dense molecular clouds which are aptly known as stellar nurseries. Because the gas and dust absorb most of the external UV radiation, the interiors

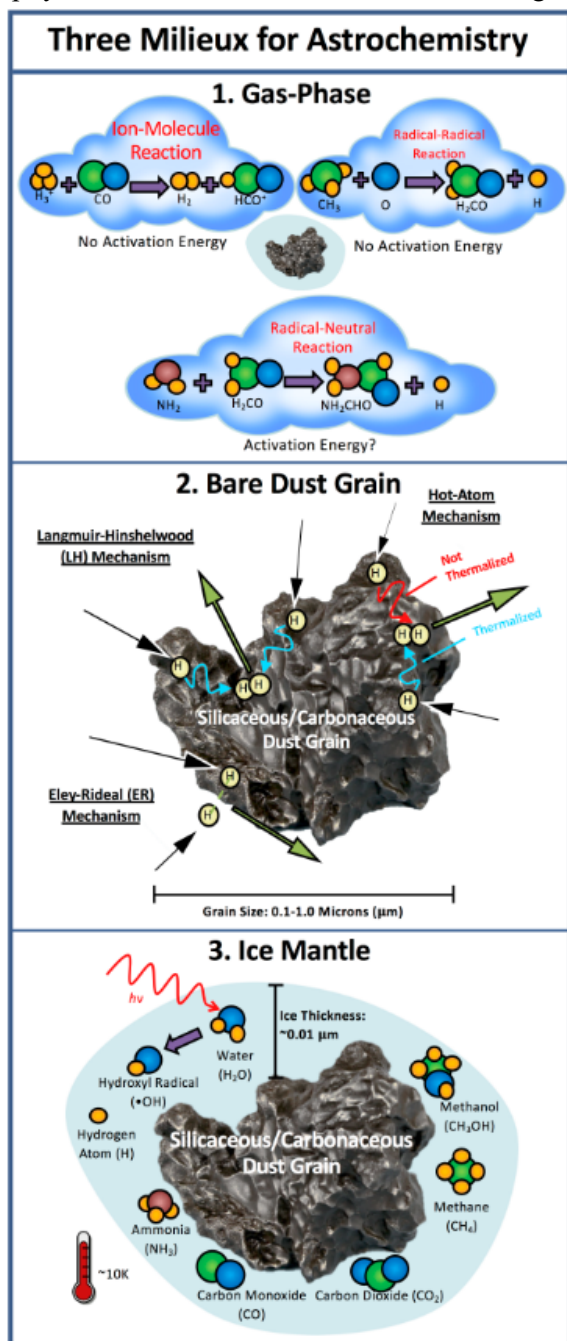


**Figure 3**

Three Environments for Interstellar Chemistry

of dark, dense molecular clouds reach temperatures as low as 10 K, ensuring the incorporation of much of the gas-phase C, N, and O into ice mantles that coat the dust grains.

Photochemistry and/or radiation chemistry of these ices produces radicals that are thought to be immobile because they cannot overcome the activation barrier for diffusion at 10 K. Further, more localized, gravitational collapse of material

onto a central dense core feeds the growth of a nascent protostar, which heats the inner regions of its surrounding envelope, thus creating the “hot” ( $\sim 100$  K), “dense” (number density  $> 10^6$  molecules/ $\text{cm}^3$ , optical depths  $\sim 10^3$ ) physical conditions in which many complex interstellar molecules (e.g., methyl formate ( $\text{HCOOCH}_3$ )) are observed. In the case

of solar-type star formation, in particular, the protostar is found to be encircled by a thin, flat, rotating structure called a protoplanetary disk.<sup>1</sup> Depending on the mass of the protostar, the transition from the cold core phase ( $\sim 10$  K) to a hot core or corino can take on the order of a million years. The warming to  $> 100$  K of individual parcels of infalling gas and dust may take  $10^4$  to several  $10^5$  years to progress. As this

warm-up stage ensues, the synthesis of complex organic molecules is thought to occur via two mechanisms: (1)

<sup>1</sup> The term “accretion disk” refers to any astrophysical disk which transports mass usually onto a compact central object. A “circumstellar disk” is any accretion disk which surrounds a star (whether young, old, low-mass, high-mass, etc.). The “protoplanetary disk” is an accretion disk around a young (usually) low-mass star ( $< 8 M_{\text{sun}}$ ) which contains the precursor material for a planetary system. (CREDIT: Catherine Walsh, University of Leeds)

barrierless radical-radical reactions following the diffusion, when the ice temperatures exceed  $\sim 30$  K, of non-thermally formed radicals, and (2) purely thermal reactions (e.g.,  $\text{NH}_3 + \text{CO}_2 \rightarrow \text{NH}_2\text{COOH}$ ) which involve an activation barrier. The latter process has been less well-explored in the literature. Desorption of the resultant new

Gas Phase Interstellar Reactions	
Reaction	Example
Cosmic-ray induced ionization	$\text{H}_2 + \text{CR} \rightarrow \text{H}_2^+$
Ion-neutral	$\text{H}_2 + \text{H}_2^+ \rightarrow \text{H}_3^+ + \bullet\text{H}$
Neutral-neutral	$\bullet\text{OH} + \text{H}_2 \rightarrow \text{H}_2\text{O} + \bullet\text{H}$
Radiative association	$\text{C}^+ + \text{H}_2 \rightarrow \text{CH}_2^+ + h\nu$
Dissociative recombination	$\text{H}_3\text{O}^+ + \text{e}^- \rightarrow \text{H}_2\text{O} + \bullet\text{H}$
Associative detachment	$\text{C}_6\text{H}^+ + \text{H} \rightarrow \text{C}_6\text{H}_2 + \text{e}^-$
Photodissociation	$\text{H}_2\text{O} + h\nu \rightarrow \bullet\text{H} + \bullet\text{OH}$
Photoionization	$\text{H}_2\text{O} + h\nu \rightarrow \text{H}_2\text{O}^+ + \text{e}^-$
Photodetachment	$\text{C}_6\text{H}^- + h\nu \rightarrow \bullet\text{C}_6\text{H} + \text{e}^-$

**Table 2**

Gas phase reaction mechanisms in the interstellar medium

important in these environments.

ice species into the gas phase may occur (1) thermally, as temperatures gradually reach between 100 and 200 K, (2) through photon/electron/ion stimulated desorption including protostellar “luminosity outbursts” caused by temporary instabilities in the accretion disk, and (3) via the exothermicity of a surface reaction (“chemical desorption”).<sup>5</sup> Mechanism (1) is usually considered the most

Ultimately, a star at the *end* of its life will eject some of the products of its nuclear fusion, enriching the interstellar medium for future star and planet formation. Mass-loss driven by winds from stars in the asymptotic giant branch (AGB) stage also provides the environment in which is formed much of the dust that permeates the interstellar medium.

## 1.2 Three Environments for Interstellar Chemistry<sup>6</sup>

The synthesis of molecules in outer space, schematically illustrated in Figure 3, may occur (1) in the gas phase, (2) on bare dust grains, or (3) in ice mantles, as described in detail below.

### 1.2.1 Gas-phase reactions

Gas-phase chemistry, important in cold ( $\sim 10$  K) cores, occurs by as many as nine different reaction mechanisms (Table 2). *Cosmic-ray-induced ionization* of gaseous molecular hydrogen leads to barrier-less *ion-neutral* gas-phase reactions, which include important interstellar processes such as proton transfer reactions. For example, the highly exothermic proton-hop gas-phase reaction



produces the triangular  $\text{H}_3^+$  ion, which played a critical role in cooling during star formation in the early universe and is hence known as the “molecule that made the universe.” Another significant gas-phase reaction mechanism involves electrons attaching to molecular cations leading to unstable molecules that subsequently dissociate spontaneously. This gas-phase reaction, known as *dissociative recombination*, has a rate constant of  $\sim 10^{-7} \text{ cm}^3 \text{ molecule}^{-1} \text{ s}^{-1}$ , which is approximately two orders of magnitude higher than the corresponding value for ion-neutral reactions. This process is often the final step in the gas-phase production of neutral species through ion-neutral reactions, whereby the protonated form of a stable molecule undergoes dissociative recombination resulting in the ejection of an H atom. Dissociative recombination of  $\text{HCNH}^+$  accounts for the observation of HCN and HNC in a nearly 1:1 ratio in cold interstellar regions, despite HNC being less stable than HCN by  $\sim 60 \text{ kJ/mol}$  at room temperature. By making D atoms available for reactions on grain surfaces, dissociative recombination of  $\text{H}_2\text{D}^+$  in dark, dense molecular clouds contributes to the high degree of deuterium fractionation,

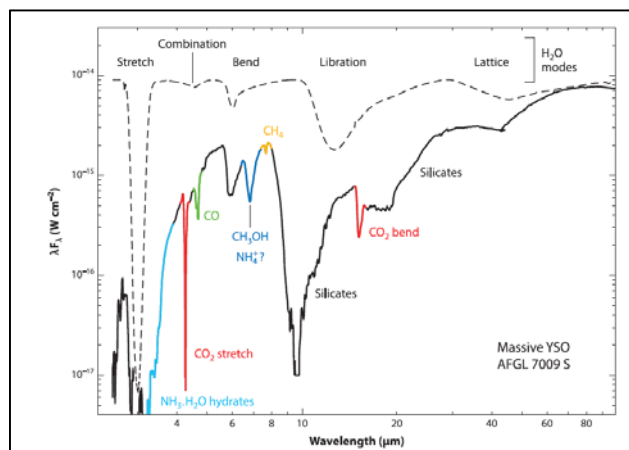


**Figure 4**

Infrared features in the massive young stellar object (YSO) AFGL 7009. The dashed line corresponds to calculated absorption features of water. Reproduced from reference 13 with permission from Annual Reviews copyright 2015.

a process in which multiply-deuterated molecules such as  $\text{ND}_3$  are produced in abundances that are orders of magnitude higher than what is expected based on the cosmic D/H elemental abundance ratio of  $1.5 \times 10^{-5}$ . The existence of methyl formate ( $\text{HCOOCH}_3$ ) and dimethyl ether ( $\text{CH}_3\text{OCH}_3$ ) in cold ( $\sim 10 \text{ K}$ ) cores has been attributed by some to the gas phase *neutral-neutral* reactions between  $\bullet\text{OH}$  radicals and methanol molecules to form methoxy radicals ( $\text{CH}_3\text{O}\bullet$ ), a reaction with an activation barrier through which quantum mechanical

tunneling<sup>m</sup> takes place more rapidly at low temperatures because of an entrance-channel complex.<sup>6</sup> Gas-phase chemistry has also been invoked to account for the formation of complex molecules such as formamide

<sup>m</sup> Chemical quantum mechanical tunneling is a process in which low-energy reactant species tunnel through the energy barrier to form products.



(HCONH<sub>2</sub>), but this is not a universally accepted mechanism.<sup>7</sup> In a limited number of cases, ion-molecule reactions may provide rapid reaction routes for more complex species (e.g., dimethyl ether (CH<sub>3</sub>OCH<sub>3</sub>)). However, such chemistry cannot explain the synthesis of all interstellar molecules. This limitation includes perhaps the most significant interstellar molecule, H<sub>2</sub>, which cannot stabilize via *radiative association* because nascent excited H<sub>2</sub> cannot redistribute excess energy between different vibrational modes.

### 1.2.2 Surface Reactions on Bare Dust Grains

The dominant formation mechanism for molecular hydrogen involves catalytic reactions on bare micron-size carbonaceous or siliceous interstellar dust grains which constitute ~ 1% by mass of dense clouds (Figure 3).<sup>8</sup> One or more of three low-temperature mechanisms account for such surface reactions which can also lead to the synthesis of “complex” molecules such as CH<sub>3</sub>OH. First, *Langmuir-Hinshelwood* (LH) reactions occur when two thermalized adsorbates diffuse, reach adjoining binding sites, react, and form products. At temperatures below ~ 10 K, a temperature regime where diffusion is inhibited, LH reactions involving atomic hydrogen may occur via quantum mechanical tunneling. Second, the *Eley-Rideal* (ER) mechanism involves a gas-phase species landing directly atop an adsorbate, initiating a chemical reaction. Third, in the *hot-atom/Harris-Kasemo* (HK) mechanism which is intermediate between LH and ER mechanisms, a non-thermalized surface species (e.g., hot precursor state) encounters a thermalized adsorbate, leading to reaction. While surface reactions on polycyclic aromatic hydrocarbons (PAHs) are associated with homogeneous catalysis, most surface reactions on dust grains correspond to heterogeneous catalysis.

### 1.2.3 Surface and Bulk Reactions of Cosmic Ices<sup>6,9, 10</sup>

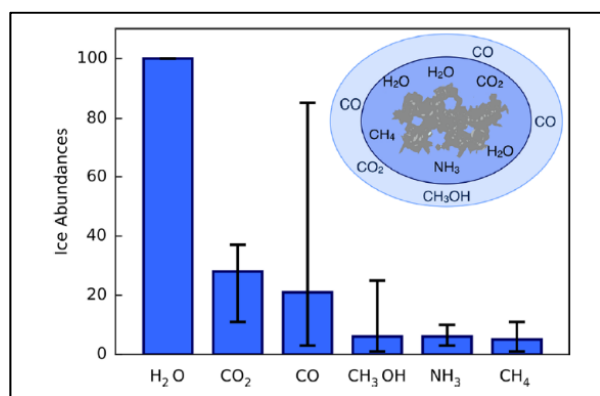
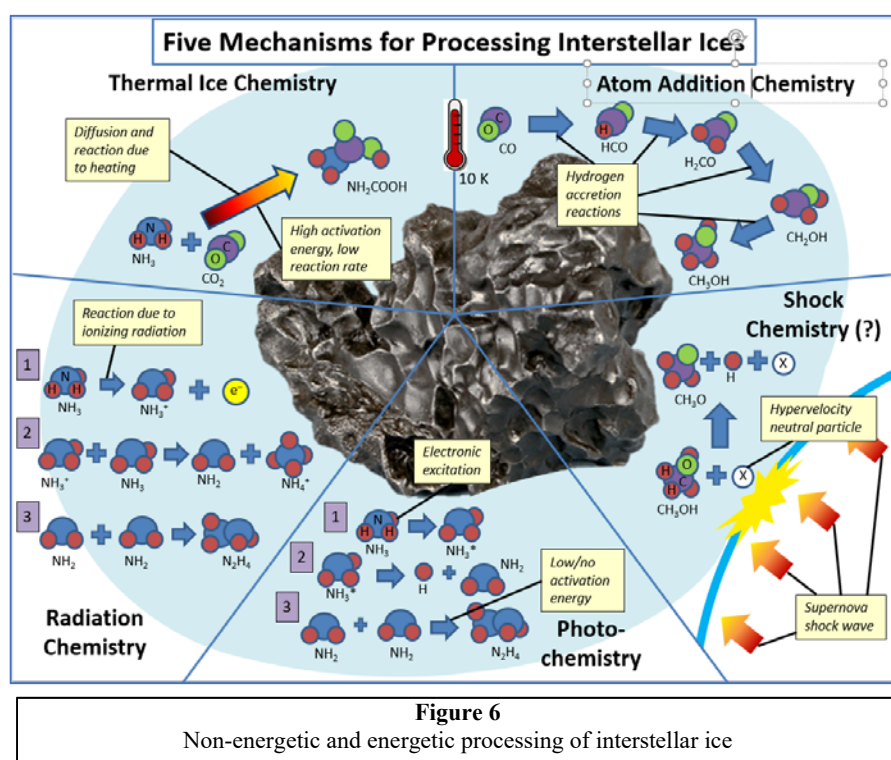


**Figure 5**

Composition of interstellar ices (Reprinted with permission from reference 9; copyright 2016 American Chemical Society)

While gas-phase reactions are not efficient enough to explain the observed abundances of most complex saturated organic molecules, recent experimental and theoretical simulations provide convincing evidence for cosmic ices being the most important environment for interstellar chemical evolution to produce prebiotic

molecules such as glycolaldehyde ( $\text{HOCH}_2\text{CHO}$ ).<sup>11</sup> In addition, energetic processing (e.g., circularly-polarized UV photons and low-energy spin-polarized secondary electrons) of cosmic ices may induce chiral selective chemistry, which may explain the “handedness” in biological molecules, one of the great mysteries of the origin of life. The 2016 discovery<sup>11</sup> of the amino acid glycine and phosphorous in the coma surrounding cometary ice is significant because (1) despite solar wind (mostly 1.5 – 10 keV protons) and cosmic ray (mostly > 1 MeV protons) bombardment, cometary ice is believed to be pristine, having not undergone any chemical changes since the birth of the solar system and (2) comets may have delivered extraterrestrial organic compounds to earth. Interestingly, in 2018, glycine formation was observed in  $\text{CO}_2:\text{CH}_4:\text{NH}_3$  ices irradiated by sub-ionization electrons.<sup>12</sup> The



existence of ice mantles surrounding interstellar dust grains has been confirmed by infrared measurements (Figure 4) made by space telescopes such as Spitzer and the Infrared Space Observatory (ISO).<sup>13</sup> This finding is not surprising given that the interiors of dark, dense molecular clouds reach temperatures as low as 10 K, ensuring the freezing of all gas-phase species<sup>o</sup> except hydrogen and

helium, leading to the formation of nanoscale ice mantles consisting of  $\text{H}_2\text{O}$ ,  $\text{CO}_2$ ,  $\text{CO}$ ,  $\text{CH}_3\text{OH}$ ,  $\text{NH}_3$ , and  $\text{CH}_4$  (Figure 5). Interestingly, the ultraviolet irradiation of interstellar ice analogs containing  $\text{H}_2\text{O}$ ,  $\text{CH}_3\text{OH}$ , and  $\text{NH}_3$  leads to the production of ribose, the central molecular subunit of RNA.<sup>14</sup> While celestial ices, some containing organics, have been detected on solar-system bodies such as asteroids (e.g., 24 Themis), comets (e.g.,

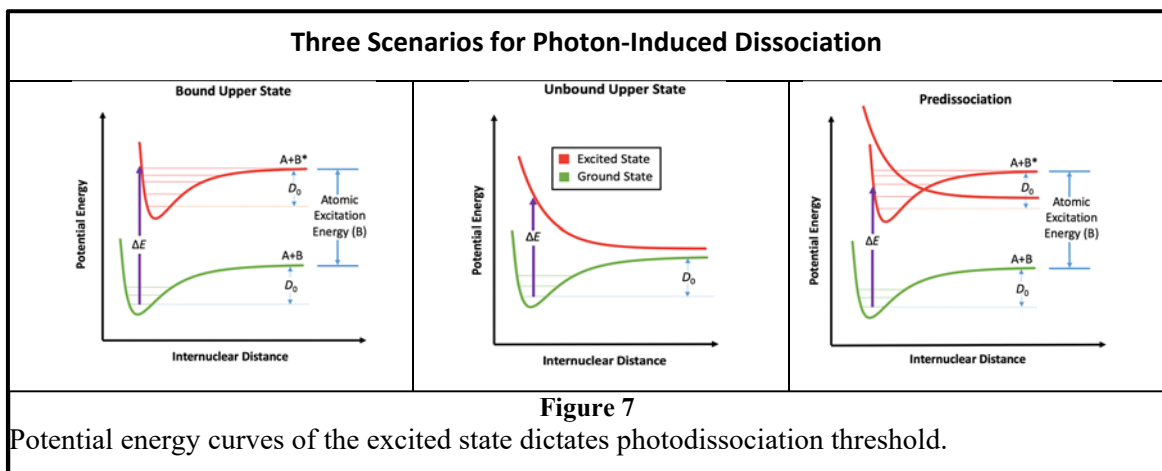
<sup>11</sup> Glycolaldehyde, the simplest monosaccharide sugar, is a precursor to RNA's ribose.

<sup>o</sup> It is important to note that a number of these gas phase species are synthesized on dust grains.

67P/Churyumov-Gerasimenko), planets (e.g., Neptune), dwarf planets (e.g., Ceres), and moons (e.g., Europa), the focus of this review is interstellar  $\sim 0.01\ \mu\text{m}$ -thick ice mantles surrounding micron-size dust grains found in prestellar cores and hot cores/corinos,<sup>p</sup> thought to be the birthplace of prebiotic molecules.

### 1.3. Five Mechanisms for Processing Interstellar Ices

The five possible mechanisms leading to extraterrestrial prebiotic molecules include both non-energetic (thermal chemistry and atom addition chemistry) and energetic (shock chemistry, photochemistry, and radiation chemistry) interstellar ice processing (Figure 6). Thermal ice chemistry<sup>15</sup> involves low-activation energy solid-state reactions between electronically-stable closed-shell molecules at cryogenic temperatures. For example, acid-base reactions (e.g., HCOOH and NH<sub>3</sub>) produce a salt (NH<sub>4</sub><sup>+</sup>HCOO<sup>-</sup>) via a proton transfer reaction.<sup>15</sup> Nucleophilic addition, elimination, and condensation reactions are other examples of thermal ice chemistry.<sup>15</sup> Atom addition chemistry<sup>16</sup> involves non-energetic atom addition reactions. Such reactions between accreting H atoms and CO molecules have been shown to form methyl formate (HCOOCH<sub>3</sub>), glycolaldehyde (HOCH<sub>2</sub>CHO), and ethylene glycol (HOCH<sub>2</sub>CH<sub>2</sub>OH).<sup>16</sup> Energetic processing (e.g., reactions and sputtering) of cosmic ices likely involves interstellar shocks including stellar winds, supernovae ejecta, and protostellar outflows which include fast jets. While evidence for gas-phase shock chemistry is well documented, studies of such collision-induced reactions in interstellar ice analogs is limited.<sup>q</sup> The competing collision-induced desorption mechanism in interstellar ice analogs, however, is an active area of research. In recent years, laboratory experiments and theoretical



calculations  
have  
suggested  
that UV  
photon-  
induced

<sup>p</sup> Interstellar ices also exist beyond the snowline in protoplanetary disks where molecules such as cyanoacetylene (HC<sub>3</sub>N) and cyclopropenylidene (c-C<sub>3</sub>H<sub>2</sub>) have been discovered.

<sup>q</sup> Collision-induced dissociation (“chemistry with a hammer”) of monolayer adsorbates such as methane on metal surfaces has been relatively well studied. Further studies are needed to understand collision induced dissociation in multilayer adsorbates.

surface and bulk processing of icy grain mantles leads to the production of radicals.<sup>9</sup> While facile light radical diffusion is possible at ~10 K,<sup>5</sup> the gradual warm-up from ~10 K to ~100 K in hot cores and hot corinos allows for heavy-radical diffusion. The subsequent barrier-less, radical-radical reactions (i.e., reactions between two open-shell species) are thought to lead to the synthesis of potential precursors of biologically important molecules.<sup>r</sup> Energetic interstellar ice processing to form prebiotic molecules via photochemistry (involving electronic excitation) and radiation chemistry<sup>s</sup> (involving electronic excitation and ionization) will be the focus of this review.

## 2. Principles of Photochemistry

According to a recent publication, “Interstellar ice photochemistry is an efficient pathway to chemical complexity in space. It is a source of prebiotic amino acids and sugars and maybe the original source of enantiomeric excess on the nascent Earth.”<sup>9</sup> As shown in equation (2):



photochemistry is defined as “the branch of chemistry which relates to the interactions between matter and photons of visible or ultraviolet light and the subsequent physical and chemical processes which occur from the electronically excited state formed by photon absorption.”<sup>17</sup> Depending on the shape of the excited state potential energy curves, photodissociation may occur via (1) a bound upper state, (2) an unbound upper state, or (3) predissociation (Figure 7). Reactions attributable solely to photochemistry are limited to those initiated by photons associated with far (deep)-UV (4.1 – 6.2 eV), near-UV (3.1 – 4.1 eV), and, occasionally, visible (1.8 eV – 3.1 eV) light.<sup>t</sup> Vacuum ultraviolet (VUV) (6.2 – 12.4 eV) light may, in addition to photochemistry, initiate radiation chemistry, as described in detail in Section 3. Sources of non-ionizing radiation, typically < 10 eV photons, responsible for photochemistry of interstellar ices include (1) interstellar radiation field (ISRF), (2) protostar blackbody radiation, and (3) secondary UV radiation (Section 4).

In contrast to thermal chemistry, which involves the ground electronic state, photochemistry concerns electronically excited states, each of which may have unique properties such as molecular geometry. The

<sup>r</sup> Some radical-radical reactions may be hindered by orientational effects.

<sup>s</sup> Note that radiochemistry refers to the application of radioactivity to the investigation of chemical problems.

<sup>t</sup> 1eV ≈ 100 kJ/mole ≈ 24 kcal/mole

electronically excited molecule may decay via primary *photophysical* and/or *photochemical* processes such as (1) luminescence (fluorescence or phosphorescence:  $A^* \rightarrow A + h\nu'$ ), (2) radiationless decay ( $A^* \rightarrow A$ ), (3) quenching ( $A^* + B \rightarrow A + B$ ), (4) photodissociation ( $A^* \rightarrow B + C$ ), (5) photoisomerization ( $A^* \rightarrow B$ ), (6) electron transfer ( $A^* + B \rightarrow A^+ + B^-$ ), (7) excitation transfer or sensitization ( $A^* + B \rightarrow A + B^*$ ), (8) bimolecular reactions ( $A^* + B \rightarrow C + D$ ), and (9) H-abstraction reaction ( $A^* + RH \rightarrow AH + R\bullet$ ). None of the reactions of a photo-excited molecule involve secondary-electron production, a signature characteristic of radiation chemistry, as described below in Section 3.

A number of core principles govern photochemistry. According to the Grotthuss-Draper law of photochemistry, only the light absorbed is effective in promoting photochemistry.<sup>u</sup> Most photochemical reactions obey the Bunsen-Roscoe law, according to which a photochemical effect is directly proportional to the total energy dose, irrespective of the time required to deliver that dose. In other words, photochemical effects, in contrast to some radiation chemical outcomes, depend on the photon fluence (photons per unit area) but not on the flux (photons per unit area per unit time). The Bunsen-Roscoe law is assumed to be valid for ice processing when extrapolating laboratory simulations (flux  $\sim 10^{14}$  photons/cm<sup>2</sup>/sec) to dark dense molecular clouds (flux  $\sim 10^4$  photons/cm<sup>2</sup>/sec). According to the Stark-Einstein law, a single molecule absorbs only one photon in the primary step of a photochemical reaction. Quantum yield,  $\Phi$ , the number of molecules of reactant R converted per photon absorbed, is used to quantify the efficiency of photochemistry reactions.

$$\Phi = \frac{\text{number of molecules of R converted}}{\text{number of photons absorbed by R}} \quad (3)$$

Because some photochemical reactions involve a chain reaction mechanism, quantum yields can be as high as  $10^6$  for reactions such as the chlorination of alkanes. In contrast, because photophysical processes such as radiative deactivation (e.g., fluorescence, phosphorescence) and nonradiative deactivation (e.g., intersystem crossing and degradation to heat by internal conversion) compete with photochemistry,<sup>v</sup> often the quantum yield

<sup>u</sup> This law may appear self-evident but note that in stimulated emission, a molecule emits radiation that it had not previously absorbed.

<sup>v</sup> Competing processes for a photoexcited molecule have time scales that range from tens of femtoseconds (e.g. internal conversion such as vibrational relaxation) to tens of seconds (phosphorescence).

can be significantly less than one. In the condensed phase, an additional competing mechanism for photochemistry is photodesorption,<sup>w</sup> a non-thermal mechanism likely responsible for the presence of gas-phase molecules around 10 K ices inside dark dense molecular clouds. Exciton<sup>x</sup> diffusion may also compete with

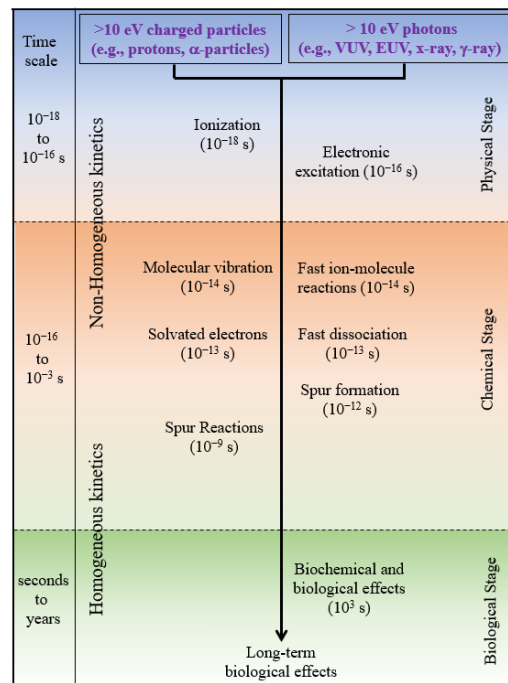


**Figure 8**

Time scales associated with radiation chemistry.

photochemistry, lowering the efficiency of photochemical reactions in the condensed phase compared to the gas phase.<sup>18</sup>

In the gas phase, photon-induced processes are said to be spin-allowed when the spin multiplicity does not change (e.g., singlet to singlet and triplet to triplet transitions). Examples of spin-allowed (4) and disallowed (5) photon-induced gas phase reactions are shown below:



Because spin-orbit coupling is proportional to the fourth power of the atomic number, spin-forbidden transitions (e.g., singlet

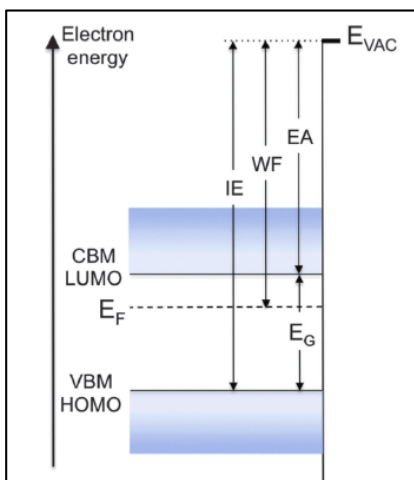


**Figure 9**

Band structure in solids. Reproduced from Ref. 21 with permission from The Royal Society of Chemistry, Copyright 2016.

to triplet) become more likely for metal-containing heavy molecules. In contrast to the gas phase, spin-forbidden photon-induced transitions are allowed in the condensed phase.<sup>19</sup>

In the condensed phase, 5–9 eV photons, those likely responsible for most solid-state photochemistry, have mean free paths ( $\lambda$ ) comparable to the thickness of interstellar ice. For example, the mean free path of 8.5 eV photons in condensed water is  $\sim 0.06$  microns, according to calculations based on the photon absorption cross-section ( $5 \times 10^{-18} \text{ cm}^2$ ) of water ice.

<sup>w</sup> Photodesorption has a typical quantum yield of  $10^{-3}$  to  $10^{-4}$  molecules per incident photon.

<sup>x</sup> An exciton is a localized electronically excited state associated with the combination of a negative electron and a positive hole (absence of electron in the valence band) bound by Coulombic attraction. Excitons exist in nonmetallic (insulators and semiconductors) crystals and move freely as a unit, allowing for energy but not charge transportation.

Because interstellar ices are  $\sim 0.01$  microns thick, most, if not all, of the ice mantle surrounding dust grains will be susceptible to photochemistry.

Multiphoton processes typically occur in laboratory settings involving lasers with high incident photon fluxes. In contrast, photochemistry of interstellar ices is likely to occur via single photon events because secondary UV photon flux is low within dark, dense molecular clouds. While in photochemistry a single  $< 10$  eV photon typically initiates one chemical reaction, in radiation chemistry a single photon/charged particle initiates a cascade of energy-loss events such as ionization, excitation, and nuclear displacement.

### 3. Principles of Radiation Chemistry

Radiation chemistry is defined as the “study of the chemical changes produced by the absorption of radiation of sufficiently high energy to produce ionization.”<sup>20</sup> The time scales corresponding to the physical, chemical, and the biological stages of radiation chemistry span approximately 26 orders of magnitude (Figure 8). Modelling radiation chemistry is extraordinarily challenging because of the associated large number of fundamental processes (Table 3).

Ionizing radiation in interstellar chemistry includes high-energy particles (e.g., MeV to TeV cosmic rays consisting mostly of protons) and high-energy photons (e.g., vacuum

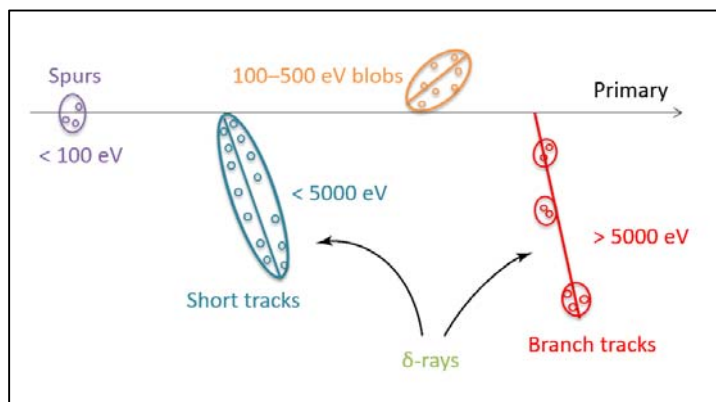


**Figure 10**

Distribution of ion-pairs and excitations in the track of a fast electron in water. Adapted from reference 23.

Fundamental Processes of Radiation Chemistry	
$AB \rightarrow AB^+ + e^-$	Direct ionization
$\rightarrow AB^{**}$	Superexcitation (direct excitation)
$\rightarrow AB^*$	Excitation (direct excitation)
$AB^{**} \rightarrow AB^+ + e^-$	Autoionization
$\rightarrow A + B$	Dissociation
$AB^+ \rightarrow A^+ + B$	Ion dissociation
$AB^+ + AB$ or $S \rightarrow$ Products	Ion-molecule reaction
$AB^+ + e^- \rightarrow AB^*$	Electron-ion recombination
$AB^+ + S^- \rightarrow$ Products	Ion-ion recombination
$e^- + S \rightarrow S^-$	Electron attachment
$e^- + nAB \rightarrow e_x^-$	Solvation
$AB^* \rightarrow A + B$	Dissociation
$\rightarrow AB$	Internal conversion and intersystem crossing
$\rightarrow BA$	Isomerization
$\rightarrow AB + h\nu$	Fluorescence
$AB^* + S \rightarrow AB + S^*$	Energy transfer
$AB^* + AB \rightarrow (AB)_2^*$	Excimer formation
$2A \rightarrow A_2$	Radical recombination
$\rightarrow C + D$	Disproportionation
$A + AB \rightarrow A_2B$	Addition
$\rightarrow A_2 + B$	Abstraction

**Table 3**

Fundamental processes of radiation chemistry. (Reproduced from reference 22 with permission from of Taylor and Francis Group, LLC, copyright 2010).

ultraviolet (VUV: 6.2 – 12.4 eV), extreme

ultraviolet (EUV: 12.4 – 124 eV), X-rays ( $> 124$

eV) and  $\gamma$ -rays (100 keV to 1 TeV)). While

ionization energy in the gaseous state is defined as

the minimum energy required to remove an electron from a ground-state atom or ion, ionization energy in the condensed phase is defined as the energy difference between the vacuum level ( $E_{\text{vac}}$ ) and the valence band maximum (VBM) (Figure 9).<sup>21</sup> Vacuum-UV (6.2 – 12.4 eV) light may initiate, in addition to photochemistry, radiation chemistry because the threshold for producing secondary electrons is lower in the condensed phase than in the gas phase for a given molecule. For example, the photoelectric emission threshold for amorphous water ice (the main constituent of cosmic ices) is  $\sim 10.2$  eV, which is smaller than water's gas phase ionization energy of 12.6 eV. This reduction in threshold energy for ionization is a general phenomenon and has been ascribed to dielectric screening of the hole produced by UV irradiation in condensed matter.

Energy transfer from the ionizing radiation to the sample is key to understanding radiation chemistry.<sup>22</sup> Interactions of electromagnetic radiation and charged particles with matter largely involve the transfer of energy to electrons and not the nuclei of the material's constituent atoms.<sup>y</sup> At energies above the ionization threshold ( $\sim 10$  eV), photon interactions with matter occur via three processes: (1) photoelectric effect, (2) the Compton effect, or (3) pair production. In contrast, protons,  $\alpha$  particles, and heavy ions<sup>z</sup> lose energy via Coulombic interactions between the ion's charge and the medium's electrons resulting in excitations and ionizations. In addition to these

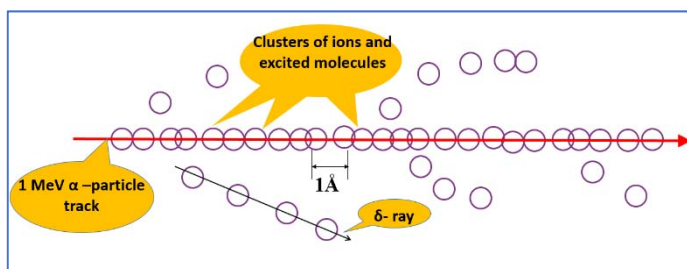


**Figure 11**  
Energy Loss by Heavy Charged Particles

two energy loss mechanisms, fast electrons can radiate energy by bremsstrahlung, the “braking” radiation emitted by a charged particle upon deceleration in the presence of an electric field.

While quantum yield is used to quantify the efficiency of photochemistry, the G-value is employed

to quantify the efficiency of reactions induced by ionizing radiation. The G-value ( $G_x$ ) is defined as the yield of species X per 100 eV absorbed energy:

$$G_x = \frac{\text{number of } \mu\text{moles of species X formed}}{\text{total energy absorbed in Joules per kg of material}} \quad (6)$$

<sup>y</sup> Processing by neutrons, another type of ionizing radiation, involves energy transfer to nuclei.

<sup>z</sup> There is some ambiguity in the definition of heavy ions. For some scientists, heavy ions refer to ionizing charged particles other than fast electrons.



Effects of radiation chemistry depend on the radiation type which is determined by linear energy transfer (LET), the rate of energy deposition by an ionizing entity per unit length of track ( $LET = -dE/dx$ ). A very rough approximation of LET can be obtained by dividing the initial energy of a particle by its mean range. Low LET (0.2 eV/nm) gamma-ray or 1 MeV electron radiolysis of water and high LET (150 eV/nm) alpha-particle irradiation of water yield remarkably different results because the former produces isolated spurs (events hundreds

Initial Stages of Water Radiolysis	
$H_2O \xrightarrow{\text{radiation}} H_2O^{\bullet+} + e^-$ and $H_2O^*$	$10^{-16}$ s
$H_2O^{\bullet+} + H_2O \rightarrow \bullet OH + H_3O^+$	$10^{-14}$ s
$H_2O^* \rightarrow H\bullet + \bullet OH, H_2 + O\bullet$	$10^{-13}$ s
$e^- + nH_2O \rightarrow e_{aq}^-$	$10^{-12}$ s

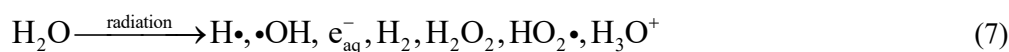
**Figure 12**

Initial stages of water radiolysis. Reproduced from ref. 24 with permission from EDP Sciences, copyright 2008.

of angstroms apart) (Figure 10)<sup>23</sup> while the latter produces dense tracks (events a few angstroms apart) which may allow for intraspur chemical reactions (Figure 11).<sup>22</sup> Both high and low LET radiation produce  $\delta$  rays which are usually

energetic electrons that cause further ionizations. The dose-rate effect<sup>aa</sup> in radiation chemistry is often associated with high linear energy transfer radiation such as heavy ions which comprise a portion of cosmic ray particles. The Bethe equation allows for the calculation of the LET for heavy ions.<sup>22</sup> In contrast to low LET radiation, high LET radiation deposits the maximum dose at the ‘‘Bragg peak’’ shortly before the track ends.

The radiation chemistry of liquid water, widely studied since the discovery of natural radioactivity around 1896, provides perhaps the best illustration of the role of LET in determining outcomes of matter-radiation interactions. The overall equation for the radiolysis of water is as follows:<sup>24</sup>



Spur Reactions in Water	
Reaction	$k$ ( $10^{10} \text{ dm}^3 \text{ mol}^{-1} \text{ s}^{-1}$ )
$e_{aq}^- + e_{aq}^- \rightarrow H_2 + 2OH^-$	0.54
$e_{aq}^- + \bullet OH \rightarrow OH^-$	3.0
$e_{aq}^- + H_3O^+ \rightarrow H\bullet + H_2O$	2.3
$e_{aq}^- + H\bullet \rightarrow H_2 + OH^-$	2.5
$H\bullet + H\bullet \rightarrow H_2$	1.3
$\bullet OH + \bullet OH \rightarrow H_2O_2$	0.53
$\bullet OH + H\bullet \rightarrow H_2O$	3.2
$H_3O^+ + OH^- \rightarrow 2H_2O$	14.3

**Figure 13**

Spur reactions in water. Reproduced from ref. 24 with permission from EDP Sciences, copyright 2008.

Initial stages of water radiolysis are characterized by four reactions involving ionization, excitation, ion-molecule reaction, bond cleavage, and solvation (Figure 12).<sup>24</sup> Spur reactions (Figure 13) which compete with diffusive escape are complete within  $10^{-7}$  s.

<sup>aa</sup> A process in which the radiation effect is not only dependent on the total energy dose, but also the time required to deliver that dose.

Degassed pure liquid water subjected to low LET radiation (e.g., X-rays) yields only small quantities of molecular products ( $\text{H}_2$  and  $\text{H}_2\text{O}_2$ ) but substantial amounts of radical species ( $\text{H}\cdot$ ,  $\cdot\text{OH}$ ,  $\text{e}_{\text{aq}}^-$ ) (Table 4). Because of the high

Products	Low-LET	High-LET
$\text{e}_{\text{aq}}^-$	0.28	0.044
$\text{H}\cdot$	0.062	0.028
$\cdot\text{OH}$	0.28	0.056
$\text{H}_2$	0.047	0.11
$\text{H}_2\text{O}_2$	0.073	0.11
$\text{H}_3\text{O}^+$	0.28	0.044

**Table 4**

Water radiolysis yields. Reproduced from ref. 24 with permission from EDP Sciences, copyright 2008.

density of ionizing events in the track of high LET radiation, radiolysis of water by alpha particles yields substantial amounts of molecular species at the expense of radicals.

In addition to affecting the physical structure of interstellar ices via sputtering, lattice defect production, and non-thermal desorption, ionizing radiation may initiate chemical reactions in interstellar ices.<sup>25</sup> The dominant

mechanism involves the interaction of high-energy radiation with molecules within ices, generating a cascade of low-energy electrons that can interact with the surface and bulk ice molecules.<sup>25</sup>

**The Importance of Low-Energy (< 20 eV) Secondary Electrons:** The interaction between high-energy

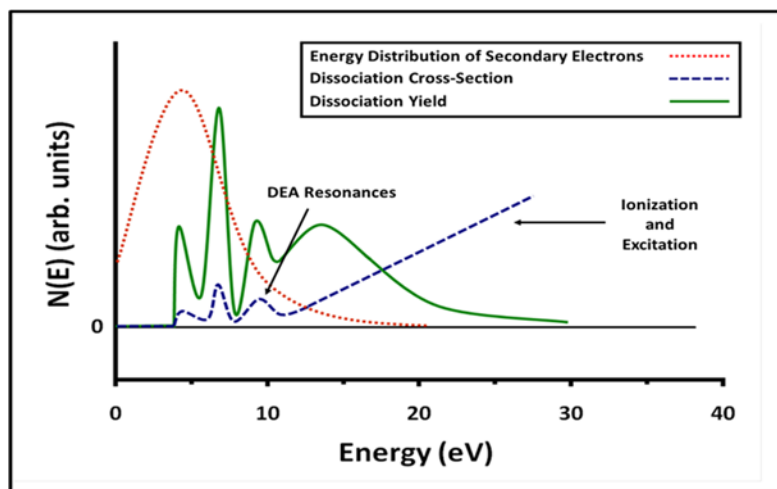


**Figure 14**

Schematic of (a) energy distribution of secondary electrons generated during a primary ionizing event (red dotted line); (b) cross-section for electron-induced dissociation for a typical molecule (blue dashed line); (c) dissociation yield as a function of electron energy for a typical molecule (green solid line). Reproduced from reference 26 with permission from Elsevier, copyright 2010

radiation (e.g., cosmic rays) and matter produces, within attoseconds, copious numbers ( $\sim 4 \times 10^4$  electrons per MeV of energy deposited) of non-thermal, secondary, low-energy (< 20 eV) electrons.<sup>26</sup> While secondary products such as excited species and ions produced from the high-energy radiation interacting with molecules cause some radiation damage, it is the secondary electron-molecule inelastic collisions that are thought to be the primary driving forces in a

wide variety of radiation-induced chemical reactions. Therefore, high-energy condensed phase radiolysis is mediated by low-energy electron-induced reactions. Electron-induced dissociations proceed via one of three initial steps: electron impact ionization, electron impact excitation, and electron attachment to form a transient

negative ion (TNI).<sup>26</sup> The electron-induced reaction yield plotted as a function of electron energy (Figure 14) evinces maxima at specific energies (resonant scattering due to electron attachment) superimposed on a smoothly increasing curve (non-resonant scattering due to electron impact ionization and/or excitation). A brief description of these three processes is given below.<sup>bb</sup>

- i. Electron-impact ionization (typically occurring at energies above  $\sim 10$  eV) of a generic molecule AB yields  $AB^{+*}$ , an excited state cation, which may undergo ion-molecule reactions or fragment to form, for example, A and  $B^{+*}$ . Because electron impact ionization is a direct non-resonant scattering process, the interaction time is short ( $\sim 10^{-16}$  seconds), on the order of the time required for the electron to traverse the molecular dimension.<sup>26</sup>
- ii. Electron-impact electronic excitation can occur at incident electron energies above  $\sim 3$  eV to yield  $AB^*$ . If the excited neutral molecule is not in a bound state,  $AB^*$  may dissociate to yield two radicals ( $\bullet A$  and  $\bullet B^*$ ).<sup>26</sup> Dipolar dissociation (DD), another channel for decay following electron-impact excitation, is the process by which the resultant excited electronic state induces ion-pair ( $A^+$  and  $B^-$ ) formation. Electron impact excitation is also a direct scattering process characterized by a short interaction time. In contrast to photon excitation, electron excitation is not a resonant process; the incident electron transfers that fraction of its energy sufficient to excite the molecule and any excess is removed by the scattered electron.<sup>26</sup>
- iii. Electron attachment to form  $AB^-$ , a transient negative ion (TNI) occurs at low electron energies, typically below  $\sim 10$  eV. The formation of a TNI is a resonant process because the final state ( $AB^{*-}$ ) is a discrete state. Dissociative electron attachment (DEA) occurs when the TNI undergoes bond scission, resulting in an anion ( $B^-$ ) in addition to a neutral atom/radical ( $A\bullet$ ). In a yield vs. electron energy plot, DEA is typically characterized by resonances below  $\sim 20$  eV.<sup>26</sup>

In contrast to photon-induced processes, electron-induced singlet-to-triplet transitions are allowed because the incident electron can be exchanged with those of the target molecule. Moreover, electrons can be captured into

---

<sup>bb</sup> Care must be taken when extrapolating results of electron-induced dissociation processes in the gas phase to the condensed phase. For example, because of the large de Broglie wavelength ( $\sim 12$  Å for a 1 eV electron) of low-energy incident electrons, the interaction of such electrons with the condensed phase must be treated theoretically as a multiple scattering problem. In addition, potential energies of both the neutral and anionic states are lowered in the condensed phase. Moreover, additional quenching processes become available in the condensed phase.

resonant negative ion states that may then dissociate. The resulting molecular fragments may then react with the parent molecule or other daughter products to yield products unique to electron irradiation. Electron-induced reactions may predominate over photon-induced reactions because of the sheer number of low-energy secondary electrons produced by high-energy irradiation. Electron impact excitation not being a resonant process also enhances electron-induced reactions vis-à-vis photon-induced reactions.<sup>cc</sup> Reaction cross-sections can be several orders of magnitude larger for electrons than for photons, particularly at incident energies corresponding to resonances associated with dissociative electron attachment.<sup>26</sup>

#### 4. Interstellar Radiation Sources

We discuss below the *possible* energetic processing sources of prestellar/hot core/hot corino ices via several interstellar radiation sources: (1) interstellar radiation field (ISRF), (2) protostar blackbody radiation, (3) secondary UV radiation, and (4) cosmic rays.

##### 4.1. Interstellar Radiation Field

The UV interstellar radiation field (ISRF),<sup>dd</sup> a photon field averaged over all types of stars, permeates all of space except within dark dense molecular clouds. The estimated UV photon flux is  $10^5$  photons/cm<sup>2</sup>/sec/Å between

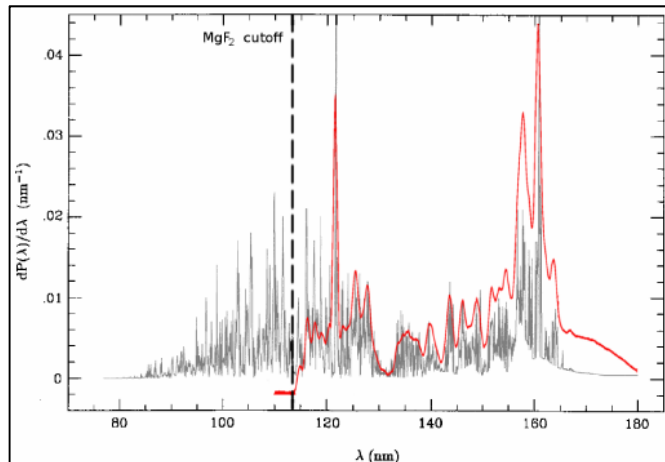


**Figure 15**

Calculated secondary UV radiation spectrum inside dark dense molecular clouds (black) and spectrum of microwave-discharge hydrogen-flow (red). Reproduced from reference 28 with permission © ESO, 2014.

912–3000 Å, which gives an integrated flux of  $\sim 10^8$  photons/cm<sup>2</sup>/sec between 4.1 and 13.6 eV.<sup>ee</sup> Except in young massive star regions, where the intensity may be enhanced by orders of magnitude, the ISRF likely does not contribute to the energetic processing of prestellar core/hot core/hot corino ices because of absorption due to dust.

##### 4.2. Protostar blackbody radiation

<sup>cc</sup> Because electron impact excitation is active over a wide range of energies, the total yields can be significant and likely increases the yield of electron driven reactions relative to photon driven processes.

<sup>dd</sup> Dust's infrared emission is the dominant component of the ISRF.

<sup>ee</sup> There is essentially no UV light above 13.6 eV in the general ISM, because the atomic H close to the stars that produce that high energy UV light will absorb all of it.

Most of the UV radiation from a protostar will be absorbed by the nearby dust. However, IR wavelengths, which can penetrate further, will heat the dust and ice with the warmest grains closest to the protostar. As a result, it is unlikely that any ices exist on grains that are able to receive substantial UV radiation. Therefore, protostellar UV radiation will likely not contribute to the energetic processing of hot core/hot corino ices.

### 4.3. Secondary UV radiation:

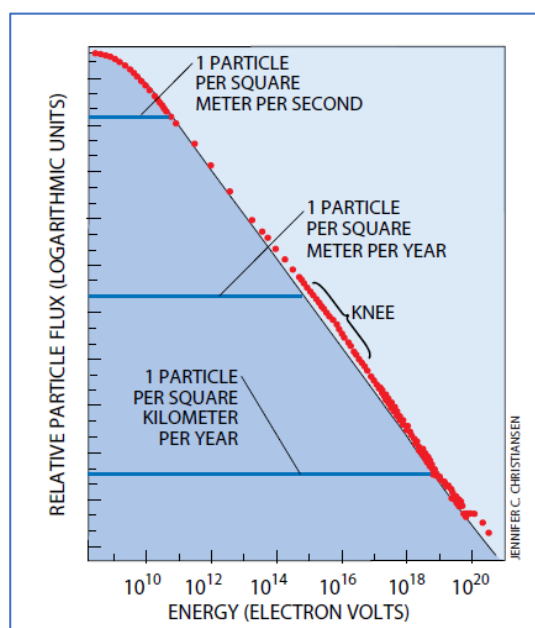


**Figure 16**

Cosmic ray flux dependence on energy. Reproduced from J. W. Cronin, T. K. Gaisser and S. P. Swordy, *Scientific American*, 276, No. 1, 1997, pp. 44-49 with permission from *Scientific American*, copyright 1997.

The source of UV light that initiates chemical reactions within dark, dense molecular clouds is thought to be local because these clouds are opaque to externally sourced UV light from the interstellar radiation field. The UV photons are believed to form in these molecular clouds where cosmic rays with energies between 10 and 100 MeV ionize molecular hydrogen to generate secondary electrons each with a mean energy around 30 eV.<sup>27</sup> These low-energy secondary electrons and primary cosmic rays can excite molecular hydrogen Lyman<sup>ff</sup> and Werner band systems whose subsequent relaxation leads to UV light emission. The UV

spectrum within the dark clouds is therefore very similar to that of microwave-discharge hydrogen-flow lamps (MDHL) in typical “photochemistry” experiments (Figure 15).<sup>28</sup> However, the flux of

secondary UV photons is estimated to be  $10^3$  photons/cm<sup>2</sup>/sec, which is significantly smaller than that of MDHL used in the laboratory to simulate UV radiation in dark dense molecular clouds.

<sup>ff</sup> Not Lyman alpha, which is a spectral line of atomic hydrogen.

#### 4.4. Cosmic Rays

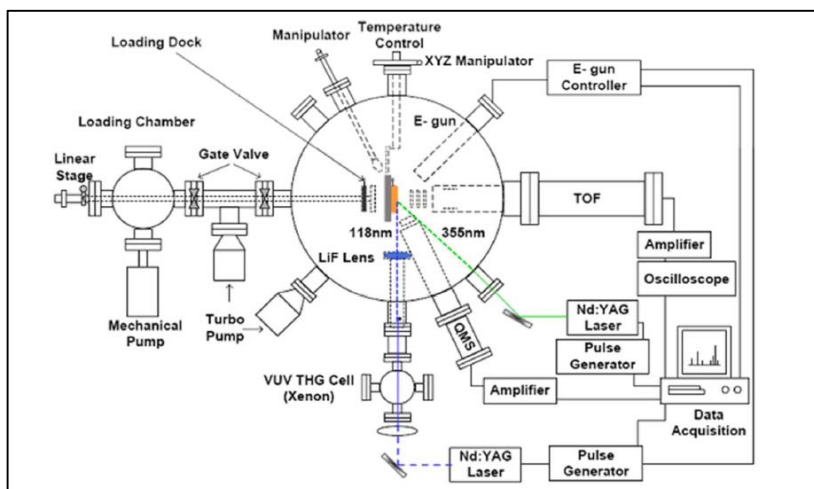


**Figure 17**

A schematic diagram of a UHV chamber with the capability of doing both stimulated and post-irradiation experiments (Reprinted with permission from reference 29; copyright 2013 American Chemical Society).

Cosmic rays whose energies range from  $10^6$  to  $10^{21}$  eV consist of relativistic charged particles ( $\sim 85\%$   $H^+$ ,  $\sim 13\%$   $He^{2+}$ ,  $\sim 1\%$  heavy bare nuclei and  $\sim 1\%$  electrons). Because the cosmic ray flux decreases sharply with increasing energy (Figure 16), only cosmic rays with energies less than  $\sim 100$  MeV make significant contributions to the energetic

processing of interstellar ices. The flux of 1 MeV protons inside dark dense clouds has been estimated to be  $\sim 1$  proton/cm<sup>2</sup>/s.<sup>13</sup>

#### 5. Irradiation Sources Used in Laboratory Studies of Cosmic Ice Analogs

Laboratory experiments to probe the energetic processing of cosmic ice analogs are typically conducted in an ultrahigh vacuum (UHV) ( $< 10^{-9}$  torr) chamber, an example of which is illustrated in Figure 17.<sup>29</sup> Although not discussed in this review, matrix isolation studies, conducted under high vacuum rather than ultrahigh vacuum conditions, offer another method to study energetic processing of cosmic ice analogs.<sup>30</sup> A comprehensive understanding of radiation/photochemistry of condensed molecular films should include both (1) stimulated desorption studies of promptly generated fragments and (2) post-irradiation analysis of the complementary retained species. Electron/photon/ion stimulated desorption experiments typically involve quadrupole mass spectrometry (QMS) or time-of-flight mass spectrometry (ToF-MS). Rotational, vibrational, and electronic states of desorbing neutrals may be characterized by resonance enhanced multiphoton ionization (REMPI). Post-irradiation analysis involves one or more techniques such as temperature programmed desorption (TPD), Fourier transform reflection absorption infrared spectroscopy (FT-RAIRS), X-ray photoelectron spectroscopy (XPS), and high-resolution electron energy loss spectroscopy (HREELS). Post-irradiation TPD involving a tunable single photon ionization coupled to a reflectron time-of-flight mass spectrometer (ReTOF-MS) is perhaps the best method to distinguish between isomers of radiolysis/photolysis products.<sup>31</sup> In addition to the in situ post-

irradiation analysis methods described above, ex situ analysis (e.g., gas chromatography–mass spectrometry (GC-MS)) can be performed on recovered refractory organic residues at room temperature and ambient conditions following irradiation at cryotemperatures under ultrahigh vacuum conditions.<sup>32</sup> Energetic processing of cosmic ice analogs is accomplished with one or more irradiation sources which are discussed below.

**5.1. Photon Sources:** Microwave-discharge hydrogen-flow lamps (MDHL) comprise approximately 90% of UV photon sources used in condensed phase studies because MDHLs best simulate the secondary UV field thought to energetically process ice mantles in dark dense molecular clouds (Figure 15). The MDHL emission spectrum is dominated by the Lyman- $\alpha$  peak (10.2 eV) and the Lyman band system of molecular hydrogen (6.9–10.9 eV) with peaks at 7.7 and 7.9 eV. MgF<sub>2</sub> and CaF<sub>2</sub> windows, typically used in MDHL sources, have photon energy cut offs of 10.9 eV and 10.0 eV, respectively. Because Lyman- $\alpha$  photons can produce secondary electrons when they interact with interstellar ices, MDHL sources typically initiate both photochemistry and radiation chemistry processes in cosmic ice analogs. In contrast to MDHL sources, irradiation with deuterium lamps (3.1–7.8 eV), tungsten halogen lamps (1.1–3.9 eV), or xenon arc lamps (0.5–6.2 eV) typically induces only photochemistry. The recently commercialized Laser-Driven Light Source (LDLS) uses a continuous wave (CW) laser to directly heat a plasma, allowing for a much higher brightness compared to traditional electrode lamps. The LDLS, with an essentially flat spectrum from 0.6–7.3 eV, has a high spectral radiance of 10–100 mW/mm<sup>2</sup>/sr/nm, allowing for the use of a monochromator. Excimer lasers are pulsed gas light sources that emit UV light at specific wavelengths (e.g., F<sub>2</sub> (7.9 eV)). Laser sources can also be used to generate tunable coherent narrow-bandwidth UV radiation by employing resonant four-wave mixing. Synchrotron radiation sources (e.g., NSRRC in Taiwan, DESIRS beamline at SOLEIL in France) produce continuous intense photon emission. In contrast to gas phase synchrotron studies which require a monochromator for high resolution, a resolution of 0.5 eV is adequate for most condensed phase studies. There is a critical need for more wavelength-dependent condensed-phase astrochemically-relevant photochemistry studies of which there have been only a few.<sup>33</sup>

**5.2. Electron guns:** The interactions of electrons with interstellar ice analogs have been studied using quasi-monoenergetic electron guns. Electron guns typically have an energy range from 1 eV to 100 keV with an energy spread < 0.5 eV, and a beam current of 1 nA–20 mA. The role of low-energy electrons in the processing of

interstellar ices by high-energy particles, such as cosmic rays, is best explored with  $< 20$  eV electrons. Such experiments require (1) low electron fluences and (2) a metal substrate to diminish the effects of film charging.<sup>gg</sup>

**5.3. Ion Sources:** The interactions of charged particles with cosmic ice analogs have been studied using multiple types of ion-beam sources including ion implanters, van de Graaff accelerators, tandem accelerators, and cyclotrons. The heavy ion cyclotron accelerator GANIL in Caen, France can produce heavy, highly charged ions that can simulate heavy-ion cosmic rays, which represent a small but significant fraction of cosmic rays in dark dense molecular clouds.

## 6. Photochemistry vs. Radiation Chemistry Experiments of Interstellar Ice Analogs

Fundamental differences between photochemistry and radiation chemistry have been detailed in sections 2 and 3. Perhaps the most obvious difference is that no matter is transparent to ionizing radiation; in contrast, pure water is transparent to visible light which is non-ionizing radiation. Unique to radiation chemistry are four phenomena: (1) production of a cascade of low-energy ( $< 20$  eV) secondary electrons which are thought to be the dominant driving force for radiation chemistry, (2) reactions initiated by cations,<sup>hh</sup> (3) non-uniform distribution of reaction intermediates, and (4) non-selective chemistry leading to the production of multiple reaction products.

A few studies have attempted to probe differences between condensed phase radiation chemistry and photochemistry relevant to the energetic processing of interstellar ices.<sup>32, 34-36,37, 38,39</sup> Although the formation of the azide ( $N_3$ ) radical from condensed nitrogen was proposed as a discriminator of radiolysis and photolysis,<sup>34</sup> the conclusion from these few studies is that the type of irradiation has little influence on product identity. However, because low-energy photons in photochemistry and low-energy electrons in radiation chemistry can both cause electronic excitation, discerning differences between the photochemistry and radiation chemistry can be challenging. Additionally, discriminating photochemistry from radiation chemistry in astrochemistry is complicated because astrophysical photon-induced chemistry studies have almost exclusively used light sources that produce  $> 10$  eV photons. While Lyman- $\alpha$  photons will not ionize condensed CO, such photons can ionize other cosmic ice constituents (e.g., water, methanol, and ammonia), generating both secondary electrons and

---

<sup>gg</sup> The influence of the metal substrate on electron/photon-induced reactions in nanoscale thin films must be carefully considered. Methods to reduce this influence (e.g., “hot-electron chemistry”) include the use of sufficiently thick films and the use of a noble gas spacer layers.

<sup>hh</sup> Electron transfer photosensitization reactions are likely not important in astrochemical environments



cations. Interestingly, irradiation of polycyclic aromatic hydrocarbon pyrene in water ice by a microwave discharge hydrogen lamp produces pyrene ( $C_{16}H_{10}$ ) cations as evidenced by post-irradiation UV spectroscopy.<sup>40</sup>

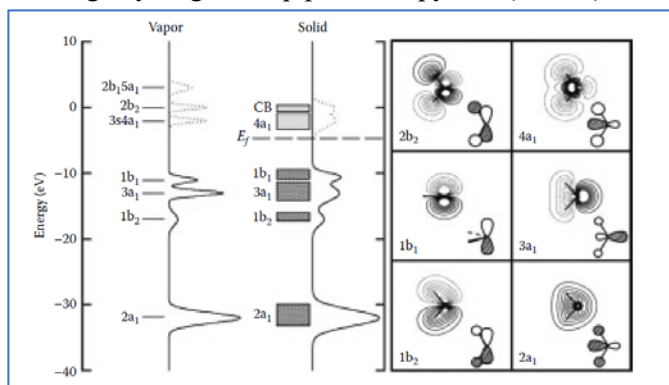


**Figure 18**

X-ray photoelectron spectra and molecular orbital contour diagrams of water. (Reproduced from reference 22 with permission from of Taylor and Francis Group, LLC, copyright 2010).

In this section we focus on the photochemistry and radiation chemistry of three (water, methanol and ammonia) pure ices which, although not faithful representatives of interstellar ices, provide an essential first step in understanding the mechanisms underlying the synthesis of complex prebiotic molecules. Our discussion includes low-energy (< 20 eV) electron-induced chemistry studies. In addition, we pay special attention to photochemistry studies conducted in the

absence of radiation chemistry.

### 6.1. Photochemistry and Radiation Chemistry of Water Ice

Understanding the photolysis and radiolysis of water ices is of fundamental importance because amorphous solid water (ASW) is the main constituent of ices found in prestellar cores/hot cores/hot corinos, the likely birthplace of prebiotic molecules.<sup>ii</sup> There are two main processes by which water ice can photodissociate:<sup>41</sup>

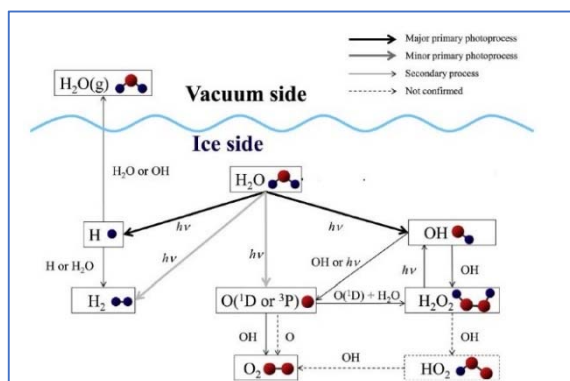
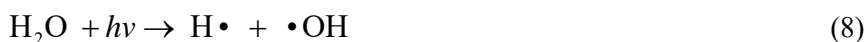


**Figure 19**

Water ice photodissociation. (The radical sign for  $H\cdot$ ,  $\cdot OH$ , and  $HOO\cdot$  are not shown) Reproduced from reference 41 with permission from Elsevier, copyright 2013.

In (9), O refers to either the ground  $^3P$  or the excited  $^1D$  oxygen atom. The water ice ultraviolet photoabsorption spectrum, consisting of a broad absorption peak centered at  $\sim 8.7$  eV and extending to a lower threshold of  $\sim 7.6$  eV, provides constraints for the photons responsible for photolysis of water.<sup>41</sup> The blue shift in the absorption peak maximum from  $\sim 7.4$  eV (gas phase) to 8.7 eV (condensed

<sup>ii</sup> Radiation-induced physical changes (e.g., compaction) in water ice will not be addressed in this review.

phase) is due partly to the greater spatial extent of the excited-state electronic wavefunction in the condensed phase. The optical absorption maximum at 8.7 eV corresponds to the  $1b_1 \rightarrow 4a_1$  transition (Figure 18).<sup>22</sup> In addition to the photoabsorption spectrum, the ionization energy also provides constraints for the photons responsible for photolysis of water. Given that the water ice ionization threshold ( $\sim 10.2$  eV) coincides with the Lyman- $\alpha$  peak, irradiation with microwave-discharge hydrogen-flow lamps will initiate radiolysis in addition to photolysis.

Studies using monochromatic photons of energy 7.9 eV, an energy within the absorption peak for water

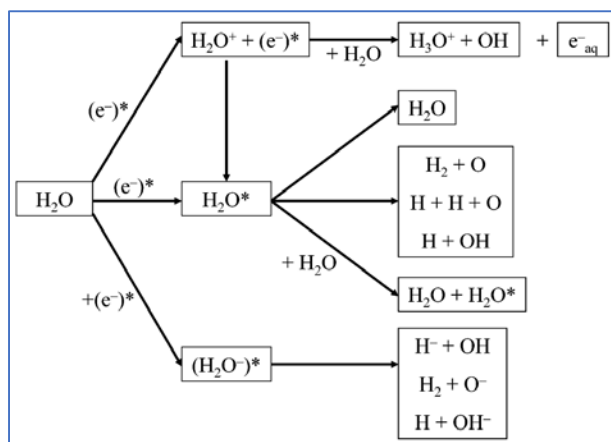


**Figure 20**

Electron-induced dissociation of water (The radical sign for  $H\bullet$  and  $\bullet OH$  are not shown) (Reprinted with permission from reference 42; copyright 2005 American Chemical Society).

ice, have detected photodesorbing products  $H\bullet$ ,  $\bullet OH$ ,  $H_2$ ,  $O\bullet$ ,  $O_2$ , and identified, through post-irradiation analysis, hydrogen peroxide ( $H_2O_2$ ).<sup>41</sup> Whereas  $H\bullet$ ,  $\bullet OH$ ,  $H_2$ , and  $O$  are direct photochemistry products of  $H_2O$  ices resulting from the two photodissociation processes described above,  $O_2$  and  $H_2O_2$  are formed through secondary processes (Figure 19). Despite a threshold of  $\sim 7.6$  eV in the

absorption spectrum of ASW, photochemistry has been detected at energies below this threshold. For example, irradiation of water ice by 6.4 eV photons leads to the

formation of some of the same products detected with 7.9 eV photons.<sup>41</sup> This sub-threshold absorption has been attributed to the ‘‘Urbach tail’’ whose origin is still a subject of debate.

In contrast with photochemistry pathways of ASW, the possible water ice radiolysis mechanisms are more diverse and less well-understood. The interaction of ionizing radiation with water produces excited and ionized water molecules and has been extensively studied for the liquid-phase. The subsequent steps in water radiolysis produce very reactive species (solvated electrons ( $e^-_{aq}$ ), hydroxide radicals ( $\bullet OH$ ), and hydrogen atoms ( $\bullet H$ )) and molecular products ( $H_2$  and  $H_2O_2$ ). While many of these same pathways are expected to be at play in the radiolysis of ASW, differences are expected due to formed micropores and defects, and the limited mobility of molecules in solid water. Figure 20 illustrates the multiple paths for the radiolysis of liquid water initiated by electrons, the main driving force for radiation chemistry.<sup>42</sup> The typical pathways for ionization (top), for

electronic excitation (middle), and for dissociative electron attachment processes (bottom) are indicated, along with the resulting products.

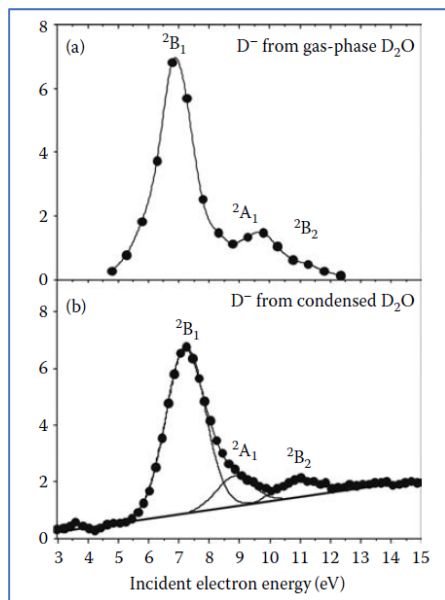


**Figure 20**

Dissociative electron attachment resonances for gaseous and solid water (Reproduced from reference 22 with permission from of Taylor and Francis Group, LLC, copyright 2010).

Laboratory radiolysis studies of water ice have been carried out using high-energy particles (e.g., 100 keV  $\text{Ar}^+$ ), soft X-ray monochromatic photons (530.7, 520, and 540 eV), and high-energy electrons (e.g., 10 keV).<sup>29</sup> Although radiation chemistry and photochemistry of water ice yield many of the same products, the underlying mechanisms are significantly more complex for radiolysis. Because of the dominant role of secondary electrons in radiation chemistry, we focus here on low-energy electron-induced water ice chemistry.

Numerous studies, some involving quantum-state resolved detection, have demonstrated that electron-stimulated desorption of water ice yields neutrals ( $\text{H}\cdot$ , O,  $\text{H}_2$ ,  $\text{O}_2$ ), anions ( $\text{H}^-$ ,  $\text{OH}^-$ , and  $\text{O}^-$ ), and cations ( $\text{H}^+$ ,  $\text{H}_2^+$  and  $\text{H}^+(\text{H}_2\text{O})_{n=2-8}$ ).<sup>22,29</sup> A 2017 study also reported the desorption of small quantities of intact  $\text{H}_2\text{O}$  during 200–300 eV electron irradiation of

amorphous solid water.<sup>43</sup> Threshold energies ( $\sim 6.5$  eV) for the electron stimulated desorption of neutral atomic oxygen and hydrogen atoms are approximately the same as that for molecular oxygen and hydrogen, suggesting that reactive scattering of hot atoms contributes to the production of these molecular species. The electron-induced formation of  $\text{D}^-$  from  $\text{D}_2\text{O}$  evinces the strong  $^2\text{B}_1$  resonance peak (6.7/7.3 eV in the gas/condensed phase) (Figure 20), corresponding to dissociative electron attachment:<sup>22</sup>



Compared to anion and neutral desorption, the energy threshold ( $\sim 22$  eV) for electron-stimulated desorption of cations ( $\text{H}^+$ ) is higher.

Temperature programmed desorption of low-energy-electron-irradiated  $\text{D}_2\text{O}$  ices also shows the formation of two additional products,  $\text{D}_2\text{O}_2$  (threshold of  $\sim 5$  eV) and the hydroperoxyl radical,  $\text{DO}_2$  (threshold of  $\sim 5.5$  eV), likely via DEA.<sup>44</sup> One possible mechanism for the formation of hydrogen peroxide is the self-reaction

of OH radicals formed in reaction (10). Both H<sub>2</sub>O<sub>2</sub> and O<sub>2</sub>, detected in water ice photolysis and radiolysis experiments, have been identified in cosmic ices such as those found on Galilean moons.

## 6.2. Photochemistry and Radiation Chemistry of Methanol Ice

	UV Photons	Electrons (≤20 eV)
•CH <sub>2</sub> OH	✓	✓
H <sub>2</sub> CO	✓	✓
HCO•	✓	
CO	✓	✓
CO <sub>2</sub>	✓	✓
CH <sub>4</sub>	✓	✓
HCOOH	✓	
CH <sub>3</sub> OCHO	✓	✓
CH <sub>3</sub> OCH <sub>3</sub>	✓	✓
HOCH <sub>2</sub> CH <sub>2</sub> OH	✓	✓
CH <sub>3</sub> OCH <sub>2</sub> OH	✓	✓
HCOCH <sub>2</sub> OH	✓	✓
CH <sub>3</sub> CH <sub>2</sub> OH	✓	✓
C <sub>2</sub> H <sub>6</sub>	✓	
CH <sub>3</sub> CHO	✓	✓
CH <sub>3</sub> COOH	✓	✓
HOCH <sub>2</sub> CO <sub>2</sub> H		✓
HOCH <sub>2</sub> CHOHCH <sub>2</sub> OH		✓

**Table 5**

Compiled from table of UV and electron studies from reference 25 with permission from Elsevier and updated (in red) to include the very recent identification of methoxymethanol as a photolysis product

Methanol (CH<sub>3</sub>OH) is found in fairly high abundances in cosmic ices. Since processing of methanol ices is thought to lead to the formation of complex organic molecules, such as methyl formate (HCOOCH<sub>3</sub>), dimethyl ether (CH<sub>3</sub>OCH<sub>3</sub>), glycolaldehyde (HOCH<sub>2</sub>CHO), acetic acid (CH<sub>3</sub>COOH), and methoxymethanol (CH<sub>3</sub>OCH<sub>2</sub>OH), which have been detected near protostars, considerable effort has been made to understand the mechanisms by which condensed methanol is processed to form these more complex molecules.

Post-irradiation studies demonstrate that UV irradiation of methanol ices yields over 15 products (Table 5).<sup>45</sup> Given that microwave-discharge hydrogen-flow lamps (dominated by the

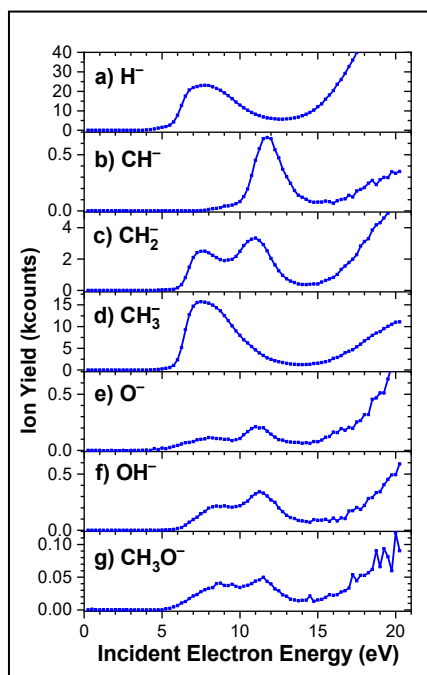
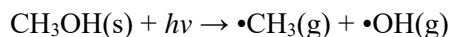


**Figure 21**

Electron stimulated desorption yield vs. electron energy for condensed methanol (reproduced from reference 25 with permission from Elsevier, copyright 2016)

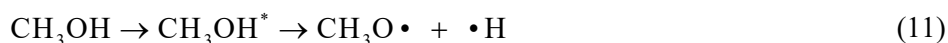
Lyman- $\alpha$  10.2 eV peak which is above condensed phase methanol's ionization threshold energy of  $\sim$ 9.8 eV) were used in three of the four studies, it is not possible to unambiguously assign all the products to photochemistry of condensed methanol.<sup>46</sup> To date, only a few photon-stimulated desorption studies of condensed methanol have been conducted using sub-ionizing photons.<sup>47</sup> In each study, the detected photodesorbed products methyl ( $\bullet$ CH<sub>3</sub>) and hydroxyl ( $\bullet$ OH) radicals were attributed to:



In addition, other photodesorbing products including carbon monoxide (CO) and formaldehyde (H<sub>2</sub>CO) were detected with a threshold of 7–8 eV.<sup>47</sup>

Radiolysis studies of condensed methanol have been conducted using

both high-energy particles (protons, He<sup>+</sup> ions, and electrons) as well as low-energy (< 20 eV) electrons. In a study comparing condensed methanol processing by high-energy (1000 eV) electrons with that by low-energy (< 20 eV) electrons, all of the products detected following high-energy-electron-processing were also detected when using only low-energy-electrons for irradiation.<sup>25</sup> This finding supports the widely accepted conjecture that high-energy condensed-phase radiolysis is mediated by low-energy electron-initiated reactions. Further, as illustrated in Table 5, the products resulting from UV photon-irradiation of methanol ices are also found as products following < 20 eV electron-irradiation of condensed methanol. While cross-sections may differ substantially, subionizing photon- and electron-induced reactions of methanol may occur via common reaction pathways involving electronic excitation:



Analogous to photodesorption experiments, electron stimulated desorption (ESD) experiments can identify products which desorb during the electron irradiation process. ESD experiments on condensed methanol have identified the following desorbing anions: H<sup>-</sup>, CH<sup>-</sup>, CH<sub>2</sub><sup>-</sup>, CH<sub>3</sub><sup>-</sup>, O<sup>-</sup>, OH<sup>-</sup>, and CH<sub>3</sub>O<sup>-</sup>.<sup>25</sup> Further, by examining their yield as a function of incident electron energy, it is possible to elucidate the dynamics through which they are formed. In particular, the peaks seen in (Figure 21) show clear dissociative electron attachment (DEA) resonances. In contrast, post-irradiation analysis of the methanol ices demonstrates no such resonances in the reaction yield versus electron energy for ethylene glycol and methoxymethanol (CH<sub>3</sub>OCH<sub>2</sub>OH).<sup>25</sup> Given the subionization threshold energies for their formation and lack of DEA resonances, electronic excitation is likely the dominant mechanism through which these products form.

When methoxymethanol was first detected in the ISM in 2017 using the Atacama Large Millimetre/submillimetre Array near a large protostar,<sup>48</sup> it was proposed that “cosmic-ray-induced chemistry may play a substantial role” in its formation because methoxymethanol was initially identified as product of electron but not UV photon-irradiation of condensed methanol. However, very recent work has determined that methoxymethanol is also a photochemistry (< 7.4 eV photons) product of condensed methanol, leading to the conclusion that it cannot be used as an indicator for electron-induced chemistry in the ISM.<sup>46</sup> Given the remaining

work needed to elucidate differences between reaction dynamics and pathways of photolysis and radiolysis of condensed methanol, it is still possible that molecular tracers which can be used to detect electron/photon dominated chemistry in the ISM will be identified.

### 6.3. Photochemistry and radiation chemistry of ammonia ice

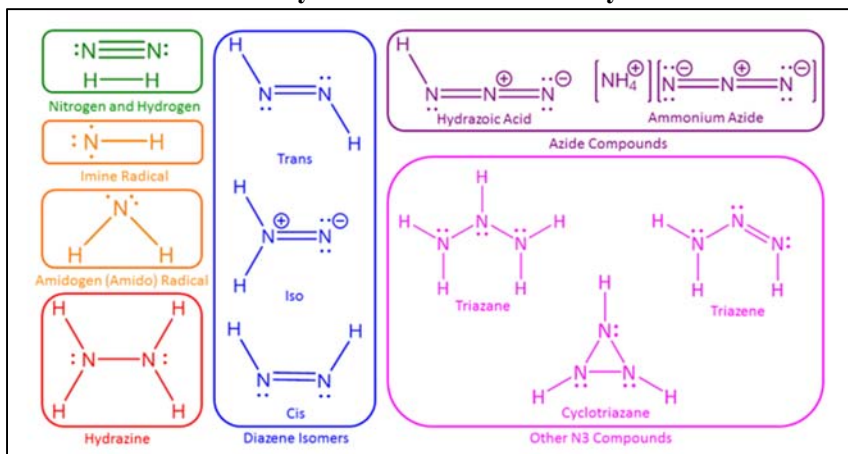


**Figure 23:**

Lewis structures of possible ammonia photolysis/radiolysis products. (Reprinted with permission from reference 49; copyright 2005 American Chemical Society).

With the possible exception of molecular nitrogen whose abundance in interstellar ices is not well constrained, ammonia is the most abundant nitrogenous compound in such ices, with an abundance of 1–10% relative to that of water. Ammonia is thus a likely precursor to prebiotic molecules such as the amino acid glycine. For

ammonia, dielectric screening reduces the ionization energy from 10.2 eV in the gas phase to  $\sim 9$  eV in the

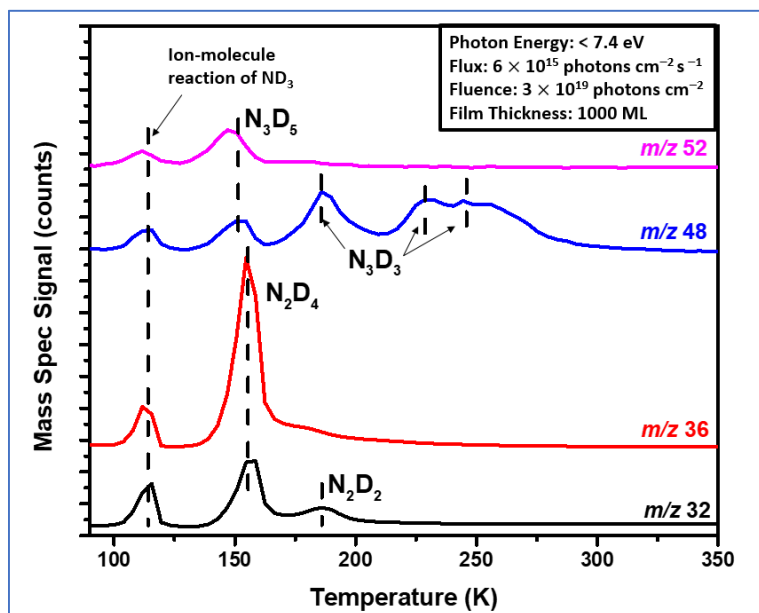


**Figure 22**

Temperature-programmed desorption of  $\text{ND}_3$  photolysis products. (Reprinted with permission from reference 49; copyright 2005 American Chemical Society).

condensed phase. Ammonia ice processing via photochemistry in the absence of radiation chemistry has been reported in three different studies.<sup>49</sup> In the first two studies, of the possible photolysis/radiolysis products of ammonia (Figure 23:), only atomic and molecular hydrogen, atomic and molecular nitrogen, ammonia, ammonium cation, and the imine (imidogen) ( $\text{NH}$ ) radical were reported as desorption products of 6.4 eV photon-irradiated pure ammonia ices. Both studies utilized photon-stimulated desorption, which

does not necessarily provide a complete understanding of condensed-phase photochemistry because inelastic

collisions may inhibit desorption of photochemistry products. Moreover, mass spectrometer-based photon-stimulated desorption experiments may be inadequate to determine product identity because all species desorb at the same temperature, in contrast to post-irradiation temperature-programmed desorption experiments. In the third study, based on post-irradiation temperature programmed desorption experiments, hydrazine ( $\text{N}_2\text{H}_4$ ), diazene (also known as diimide and diimine) ( $\text{N}_2\text{H}_2$ ), triazane ( $\text{N}_3\text{H}_5$ ), and one or more isomers of  $\text{N}_3\text{H}_3$  were identified as pure photochemistry products of ammonia (Figure 22).<sup>49</sup> Although photochemistry is cited as a dominant mechanism for the synthesis of prebiotic molecules in interstellar ices, this is one of the first astrochemically-relevant studies that has found unambiguous evidence for condensed-phase chemical synthesis induced by photons in the absence of ionization. Interestingly, the same photochemistry products ( $\text{N}_2\text{H}_2$ ,  $\text{N}_2\text{H}_4$ ,  $\text{N}_3\text{H}_3$ , and  $\text{N}_3\text{H}_5$ ) were previously identified as radiolysis products of ammonia.<sup>50</sup>

## 7. Theory/Calculations/Simulations Relevant to Energetic Processing of Interstellar Ices

The chemistry associated with the energetic processing of interstellar ice has been included in astrochemical models in only a very limited way over the past few decades, and until recently the emphasis was mostly on UV-induced photodissociation. New modeling treatments have now been developed that take account of radiolysis induced by cosmic rays, allowing gas-phase chemistry, diffusive grain-surface chemistry, and ice-mantle radiolysis to be simulated in tandem using rate equation-based modeling methods. This treatment of cosmic ray-induced radiolysis allows the net chemical effects of ionization, excitation,<sup>jj</sup> and recombination in the ice to be taken into account, without requiring the explicit calculation of electronic or primary-ion trajectories, or the modeling of each electron's interactions with individual molecules in the ice. Such an approach is computationally efficient enough to allow astrochemical systems to be modelled over astronomical timescales (i.e., thousands to millions of years).

### 7.1. Gas-grain astrochemical models

Most modern computational models of the chemistry of dark interstellar clouds include a coupled gas-phase and grain-surface chemistry that allows the gradual build-up of dust-grain ice mantles to be simulated over

---

<sup>jj</sup> For mostly historical reasons, astrochemical models of photochemistry do not take into account the interactions of excited species with other species.

astronomical timescales. Most ice formation results from the deposition of atoms and simple molecules from the gas phase, followed by additional reactions on the grain surfaces, to form simple hydrides, including water. Many recent simulations have also made use of the so-called “three-phase”<sup>kk</sup> approach,<sup>51</sup> which treats the surface layer(s) of the ice mantle as physically and chemically distinct from the bulk ice beneath, with some studies including an explicit bulk-ice chemistry.<sup>52</sup> Although more-complex stochastic treatments exist to deal with the ice chemistry alone,<sup>6</sup> simulations of coupled gas, surface, and bulk-ice chemistry in star-forming cores usually involve the solution to a set of rate-equations governing each reaction or process, providing time-dependent populations for all species in each physical phase. Photodissociation rates in the ice are usually adapted directly from gas-phase rates. For smaller molecules, calculations are based on measured and calculated photodissociation cross-sections and the cosmic ray-induced UV spectrum. For larger molecules, the rates are simply order-of-magnitude approximations. This approach allows ice photochemistry to be simulated as two independent processes: 1) production of ground state radicals via cosmic ray-induced UV photolysis, followed by 2) thermal bulk diffusion and (usually) association of those radicals. Thus, in their modeling of photochemistry, these simulations make no explicit consideration for ionization or reaction/diffusion of excited products.<sup>ll</sup> These rate-equation based three-phase modeling treatments of UV-induced photochemistry have been especially successful in broadly reproducing the abundances of complex organic molecules observed toward hot cores/corinos. Predictions have also been made using such models concerning the putative interstellar abundances of simple, but potentially important prebiotic molecules including amino acids.<sup>52</sup> Experimental studies have gone further, with a recent study indicating that UV-induced photochemistry in ice mixtures composed of simple hydrides may have allowed sugars to have formed during the disk stage of stellar evolution.<sup>14</sup> Astrochemical models of such photo-processing have not yet reached this level of chemical complexity, but the modeling tools required to do so are well enough developed in principle.

In spite of the apparent success of these models in reproducing observed abundances of complex molecules within warm regions of star formation, recent detections of several complex organic molecules (e.g. methyl formate ( $\text{HCOOCH}_3$ ) and dimethyl ether ( $\text{CH}_3\text{OCH}_3$ )) in cold ( $\sim 10$  K), dense cores, albeit in smaller abundance

---

<sup>kk</sup> ice surface and grain surface are treated as the same phase.

<sup>ll</sup> Diffusion of excited products is often called “non-thermal diffusion.”



than in hot cores, have led to the search for alternative mechanisms for complex molecule production through cold or non-thermal mechanisms, including radiolysis by cosmic rays. Attempting to explain the origin of these cold-core molecules has been a driving force for a workable computational radiolysis treatment that can be incorporated into existing astrochemical models.

## 7.2. Monte Carlo modeling treatments of interstellar cosmic ray-induced radiolysis

Although cosmic-ray impacts have sometimes been included in models as a heating mechanism for the purpose of ejecting volatile species from icy dust grains, until recently models have given little consideration to the chemical effects resulting from the radiolysis of interstellar ices. While two 2018 studies now provide an outline for a general methodology to implement radiolysis into rate equation-based models, specifically for cosmic-ray interactions with interstellar ices,<sup>53</sup> this work was informed by a detailed condensed phase radiolysis study published in 2017 that used Monte Carlo techniques appropriate for the stochastic (random) collisions between energetic particles (protons) and the target species (O<sub>2</sub> in ice).<sup>54</sup>

The Monte Carlo approach<sup>54</sup> breaks down the radiolysis process into several steps, which can be assumed to occur sequentially: (i) the formation of track structure, including calculations of the number of inelastic collisions (i.e., collisions with electrons in the target material) and the formation of track structure for the secondary electrons produced through such collisions (see Figure 25); (ii) physicochemical processes, which include ionization and electronic excitation by secondary electrons; (iii) non-homogeneous chemistry resulting from the effects of excitation and ionization, including recombination with electrons and/or molecular dissociation following electron attachment; and (iv) homogeneous/thermal chemistry based on the products of the earlier stages. The Monte Carlo simulations<sup>54</sup> considered 100 keV proton impacts onto a crystal lattice of (initially) O<sub>2</sub>, and explicitly traced each reactant and product over time. This model took account of atomic oxygen, O<sub>2</sub>, and ozone (O<sub>3</sub>) excitation and ionization by protons and secondary electrons, as well as the production of atomic or molecular anions via either electron attachment to atomic oxygen or dissociative electron attachment with O<sub>2</sub> and O<sub>3</sub>. It employed a substantial chemical-reaction-network, with excited species allowed to react with their immediate neighbors. Ion-neutral reactions were not included, on the assumption that cations are quickly neutralized by combination with anions or sub-excitation secondary electrons. The nuclear (elastic) stopping cross-sections for protons were calculated using standard methods already included in models such as

TRIM (Transport of Ions in Matter), while electronic (inelastic) cross-sections for ionization and excitation were

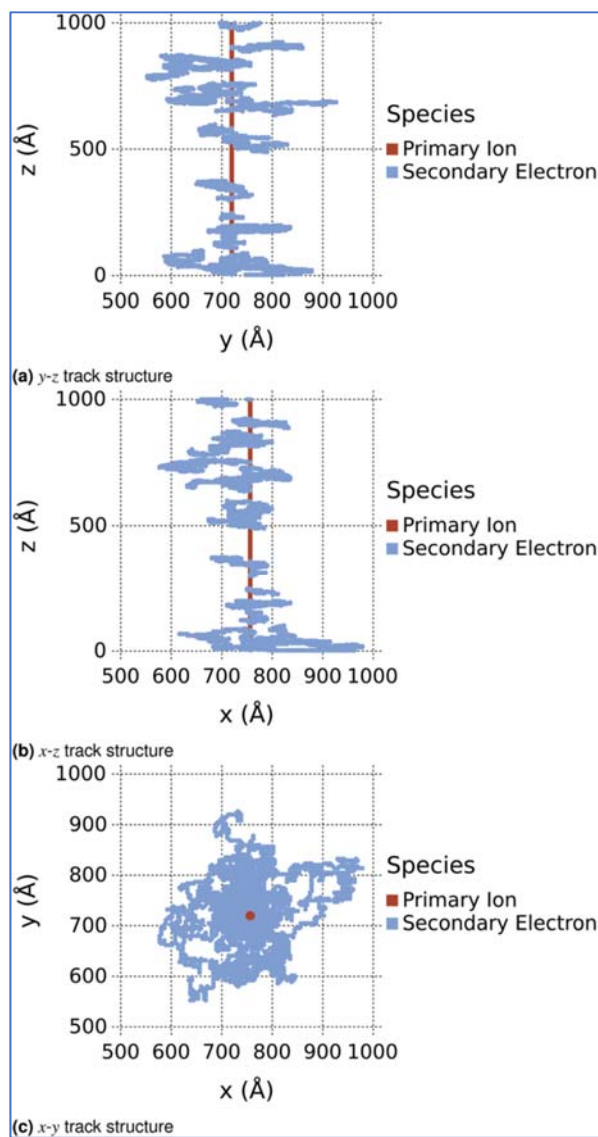


**Figure 24**

Sample track structure in which a proton collides with a pristine O<sub>2</sub> ice. Reproduced from Ref. 54 with permission from The Royal Society of Chemistry, copyright 2017.

calculated using semi-empirical formulae based on the excitation/ionization energies, as well as empirical parameters tuned by experiment. The results are in good agreement with the production of ozone obtained in experimental investigations of the same system, suggesting that Monte Carlo track simulations for solid-phase water (which would be more directly applicable to interstellar ice compositions) would also yield useful data.

Indeed, the incorporation of all of the above processes associated with radiolysis into full simulations of interstellar chemistry would be informative. However, while Monte Carlo track-simulation methods are useful in explaining well-controlled laboratory experiments with limited numbers of chemical species, the large computational costs associated with such models means that full-scale adoption of these techniques into existing treatments of interstellar chemistry remains a long way off. Radiolysis of interstellar ices must ultimately be considered within a larger context which includes other thermal and non-thermal processes influencing the ice composition over periods as

long as one million years.

To this end, the same authors developed a simplified rate-equation modeling treatment for cosmic ray-driven radiation chemistry that will allow incorporation into standard astrochemical models, and which will facilitate the testing of these mechanisms on a more even footing with other interstellar chemical processes.<sup>53</sup>

### 7.3. Rate-based modeling treatments of interstellar cosmic ray-induced radiolysis

The new rate-equation approach<sup>53</sup> makes the same major approximation as the Monte Carlo technique<sup>54</sup> that all ionization events result in rapid<sup>mm</sup> charge neutralization (followed by dissociation and/or excitation), but includes a further assumption that all such collisional ionization or excitation events (caused either by the primary ion or secondary electrons) are sufficiently far apart in the bulk ice that the excited products interact only with nearby, unexcited ice constituents. At the high energies (100 MeV to 1 GeV) characteristic of cosmic rays, the interaction cross-sections for both primary and secondary impactors are likely to be low, and thus the assumption of the isolated production of excited state species is reasonably accurate. In addition, in this rate-equation based model, electrons produced by cosmic-ray induced ionization are only allowed to recombine with cations. This rate-equation based model does not account for two effects (1) the chemical influence of electrons and cations produced by UV-induced ionization and (2) collision on ices of thermal and nonthermal electrons from the gas phase.

When the cold-core radiolysis rate-equation-based simulations were tested explicitly in a large astrochemical model,<sup>53</sup> taking into account “chemical desorption,”<sup>55</sup> the abundances of a number of gas-phase species such as methyl formate were enhanced compared to that obtained assuming only photochemical processing.<sup>mm</sup> These findings suggest that the radiolytic production of excited-state species that can undergo rapid reaction may contribute to the synthesis of complex organic molecules in cold (~10 K) cores.

#### 7.4. Consideration of charge in ice models

While interstellar chemical models explicitly trace the abundances of *gas-phase* electrons, singly-ionized cations, and a small selection of anions, there are currently no astrochemical models (known to the authors) that includes a complete treatment of ions or electrons within the ices. The above-described Monte Carlo model of the radiolysis of O<sub>2</sub> ice models the behavior of secondary electrons during an initial track-formation stage, and allows anions and cations to react subsequently. But this treatment omits the reactions of either cations or anions with neutral species. The rate-equation based astrochemical radiolysis treatment that is based on the Monte Carlo treatment largely omits the influence of low-energy electrons on the chemistry, because free electrons are assumed to rapidly recombine with cations, and no ionic abundances are explicitly calculated in those models.

---

<sup>mm</sup> in relation to the much slower diffusive (thermal) chemistry

<sup>nn</sup> We note, however, that the cosmic ray/UV flux within hot cores and cold cores should not be significantly different.

The influence on ice chemistry of low-energy electrons, produced either by radiolysis or indeed by UV-induced ionization, thus remain to be explicitly tested in astrochemical treatments.

Furthermore, in chemical networks used for typical rate equations-based astrochemical models, the interaction of gas phase electrons and positive (atomic and molecular) ions with ice-surface molecules are not considered in any meaningful way. To date, there have been few studies of reactions related to such processes for species of astronomical interest. The influence of gas- and solid-phase cations on solid-phase interstellar chemistry may therefore be a topic of considerable interest in the future.

## 8. Conclusions and Future Studies

Astrochemistry discoveries such as the first chiral molecule, propylene oxide, in space (2017), the first radioactive molecule,  $^{26}\text{AlF}$ , in space (2018), the detection of complex macromolecular organics coming from Enceladus, an extraterrestrial ice world (2018), the formation of 2-deoxyribose, the sugar that makes up the backbone of DNA, by the energetic processing of cosmic ice analogs (2018) often make headline news. Revolutionary observational tools (first ALMA results published in 2012), innovative very bright broad-band sub-ionization photon sources (available since 2012), and novel computational methods that consider radiation chemistry (published in 2018) have provided new insights into the energetic processing of interstellar ices. Despite several fundamental differences in reaction mechanisms between radiation chemistry and photochemistry, the limited number of *qualitative* cosmic-ice analog comparison studies conducted to date have essentially found the same reaction products. While these experimental results may suggest that electronic excitation, common to both types of energetic processing, is the dominant reaction-initiating mechanism, the use of  $> 10$  eV photons in studying “photochemistry” may contribute to uncertainty in some of the reported results. Many more *quantitative* studies that probe low-energy ( $< 10$  eV) electron-, photon-, ion-induced chemistry studies are needed to evaluate the relative importance of photochemistry and radiation chemistry in astrochemistry. A comprehensive experimental comparison should include both (1) stimulated desorption studies of promptly generated fragments and (2) post-irradiation analysis of the complementary retained species. Importantly, theoretical methods to study radiation chemistry need to incorporate the chemical effects of low-energy ions and electrons in ice chemistry. Together with new observational tools (James Webb space telescope to be launched in 2021) such studies will provide a more detailed understanding of how prebiotic molecules are synthesized in cosmic ices surrounding

interstellar dust grains found near star-forming regions of the universe. Such studies may help us better understand the initial stages of the genesis of life.

### Acknowledgments

This work was supported by grants from the National Science Foundation (NSF grant number CHE-1465161), Wellesley College (Faculty awards and Brachman Hoffman small grants), and Clark University (Sherman Fairchild Summer Scholars Program and the Physics Department). RTG acknowledges support from the NASA Astrophysics Theory (ATP), Astrophysics Research and Analysis (APRA), and Emerging Worlds (EW) programs. We gratefully acknowledge several useful discussions with Dr. Andrew Bass, Dr. Chris Shingledecker, Dr. Michel Nuevo, Dr. Gustavo Cruz Diaz, and Dr. Edith Fayolle.

1. J. Berkowitz, *The Stardust Revolution*, Prometheus Books, New York, 2012.
2. E. F. van Dishoeck, E. Herbst and D. A. Neufeld, *Chem. Rev.*, 2013, **113**, 9043-9085.
3. D. Skouteris, F. Vazart, C. Ceccarelli, N. Balucani, C. Pizzarini and V. Barone, *Monthly Notices of the Royal Astronomical Society: Letters*, 2017, **468**, L1-L5.
4. N. Goldman, E. J. Reed, L. E. Fried, I. F. William Kuo and A. Maiti, *Nature Chemistry*, 2010, **2**, 949.
5. Y. Oba, T. Tomaru, T. Lamberts, A. Kouchi and N. Watanabe, *Nat. Astron.*, 2018, **2**, 228-232.
6. E. Herbst, *Int Rev Phys Chem*, 2017, **36**, 287-331.
7. L. Song and J. Kastner, *Physical Chemistry Chemical Physics*, 2016, **18**, 29278-29285.
8. G. Vidali, *Chem. Rev.*, 2013, **113**, 8762-8782.
9. K. I. Öberg, *Chemical Reviews*, 2016, **116**, 9631-9663.
10. R. T. Garrod and S. L. W. Weaver, *Chem. Rev.*, 2013, **113**, 8939-8960.
11. K. Altwegg, H. Balsiger, A. Bar-Nun, J. J. Berthelier, A. Bieler, P. Bochsler, C. Briois, U. Calmonte, M. R. Combi, H. Cottin, J. De Keyser, F. Dhooghe, B. Fiethe, S. A. Fuselier, S. Gasc, T. I. Gombosi, K. C. Hansen, M. Haessig, A. Jackel, E. Kopp, A. Korth, L. Le Roy, U. Mall, B. Marty, O. Mousis, T. Owen, H. Reme, M. Rubin, T. Semon, C. Y. Tzou, J. H. Waite and P. Wurz, *Science Advances*, 2016, **2**, e1600285.
12. S. Esmaili, A. D. Bass, P. Cloutier, L. Sanche and M. A. Huels, *Journal of Chemical Physics*, 2018, **148**, 8.
13. A. C. A. Boogert, P. A. Gerakines and D. C. B. Whittet, in *Annual Review of Astronomy and Astrophysics, Vol 53*, eds. S. M. Faber and E. VanDishoeck, 2015, vol. 53, pp. 541-581.
14. C. Meinert, I. Myrgorodska, P. de Marcellus, T. Buhse, L. Nahon, S. V. Hoffmann, L. L. d'Hendecourt and U. J. Meierhenrich, *Science*, 2016, **352**, 208-212.
15. P. Theule, F. Duvernay, G. Danger, F. Borget, J. B. Bossa, V. Vinogradoff, F. Mispelaer and T. Chiavassa, *Advances in Space Research*, 2013, **52**, 1567-1579.
16. H. Linnartz, S. Ioppolo and G. Fedoseev, *Int Rev Phys Chem*, 2015, **34**, 205-237.
17. B. Wardle, *Principles and Applications of Photochemistry*, Wiley, Chichester, UK, 2009.
18. M. McCoustra and J. Throrer, in *Encyclopedia of Interfacial Chemistry: Surface Science and Electrochemistry*, ed. K. Wandelt, Elsevier, 2018, vol. 2, p. 383.
19. V. E. Bondybey, A. M. Smith and J. Agreiter, *Chem. Rev.*, 1996, **96**, 2113-2134.
20. R. J. Woods, in *Environmental Applications of Ionizing Radiation*, ed. R. D. C. William J. Cooper, Kevin E. O'Shea, John Wiley & Sons. Inc, 1998, p. 752.
21. A. Kahn, *Mater. Horiz.*, 2016, **3**, 7-10.

22. Y. Hatano, Y. Katsumura and A. Mozumder, *Charged Particle and Photon Interactions with Matter : Recent Advances, Applications, and Interfaces*, Chapman and Hall/CRC, Baton Rouge, UNITED STATES, 2010.
23. M. Burton, *Chem. Eng. News*, 1969, **47**, 86-97.
24. J. Belloni, M. Mostafavi, T. Douki and M. Spothem-Maurizot, *Radiation chemistry - From basics to applications in material and life sciences*, 2008.
25. M. C. Boyer, N. Rivas, A. A. Tran, C. A. Verish and C. R. Arumainayagam, *Surface Science*, 2016, **652**, 26-32.
26. C. R. Arumainayagam, H. L. Lee, R. B. Nelson, D. R. Haines and R. P. Gunawardane, *Surf Sci Rep*, 2010, **65**, 1-44.
27. R. Gredel, S. Lepp, A. Dalgarno and E. Herbst, *Astrophys. J.*, 1989, **347**, 289-293.
28. G. Cruz-Diaz, G. Caro, Y. Chen and T. Yih, *Astronomy & Astrophysics*, 2014, **562**, A119.
29. C. J. Bennett, C. Pirim and T. M. Orlando, *Chem. Rev.*, 2013, **113**, 9086-+.
30. V. I. Feldman, S. V. Ryazantsev, E. V. Saenko, S. V. Kameneva and E. S. Shiryaeva, *Radiation Physics and Chemistry*, 2016, **124**, 7-13.
31. A. Bergantini, P. Maksyutenko and R. I. Kaiser, *Astrophysical Journal*, 2017, **841**, 24.
32. C. K. Materese, D. P. Cruikshank, S. A. Sandford, H. Imanaka and M. Nuevo, *Astrophysical Journal*, 2015, **812**, 9.
33. J. H. Fillion, E. C. Fayolle, X. Michaut, M. Doronin, L. Philippe, J. Rakovsky, C. Romanzin, N. Champion, K. I. Oberg, H. Linnartz and M. Bertin, *Faraday Discuss*, 2014, **168**, 533-552.
34. R. L. Hudson and M. H. Moore, *Astrophysical Journal*, 2002, **568**, 1095-1099.
35. P. A. Gerakines, M. H. Moore and R. L. Hudson, *J. Geophys. Res.-Planets*, 2001, **106**, 33381-33385.
36. P. A. Gerakines, M. H. Moore and R. L. Hudson, *Icarus*, 2004, **170**, 202-213.
37. G. M. M. Caro, E. Dartois, P. Boduch, H. Rothard, A. Domaracka and A. Jimenez-Escobar, *Astronomy & Astrophysics*, 2014, **566**, A93.
38. A. Ciaravella, Y. J. Chen, C. Cecchi-Pestellini, A. Jimenez-Escobar, G. M. M. Caro, K. J. Chuang and C. H. Huang, *Astrophysical Journal*, 2016, **819**, 12.
39. A. Ciaravella, G. M. Caro, A. J. Escobar, C. Cecchi-Pestellini, S. Giarrusso, M. Barbera and A. Collura, *Astrophys J Lett*, 2010, **722**, L45-L48.
40. J. Bouwman, D. M. Paardekooper, H. M. Cuppen, H. Linnartz and L. J. Allamandola, *Astrophysical Journal*, 2009, **700**, 56-62.
41. A. Yabushita, T. Hama and M. Kawasaki, *J. Photochem. Photobiol. C-Photochem. Rev.*, 2013, **16**, 46-61.
42. B. C. Garrett, D. A. Dixon, D. M. Camaioni, D. M. Chipman, M. A. Johnson, C. D. Jonah, G. A. Kimmel, J. H. Miller, T. N. Rescigno, P. J. Rossky, S. S. Xantheas, S. D. Colson, A. H. Laufer, D. Ray, P. F. Barbara, D. M. Bartels, K. H. Becker, H. Bowen, S. E. Bradforth, I. Carmichael, J. V. Coe, L. R. Corrales, J. P. Cowin, M. Dupuis, K. B. Eisenthal, J. A. Franz, M. S. Gutowski, K. D. Jordan, B. D. Kay, J. A. LaVerne, S. V. Lyman, T. E. Madey, C. W. McCurdy, D. Meisel, S. Mukamel, A. R. Nilsson, T. M. Orlando, N. G. Petrik, S. M. Pimblott, J. R. Rustad, G. K. Schenter, S. J. Singer, A. Tokmakoff, L. S. Wang, C. Wittig and T. S. Zwier, *Chem. Rev.*, 2005, **105**, 355-389.
43. A. G. M. Abdulgalil, A. Rosu-Finsen, D. Marchione, J. D. Thrower, M. P. Collings and M. R. S. McCoustra, *Acs Earth and Space Chemistry*, 2017, **1**, 209-215.
44. X. N. Pan, A. D. Bass, J. P. Jay-Gerin and L. Sanche, *Icarus*, 2004, **172**, 521-525.
45. K. Oberg, R. Garrod, E. van Dishoeck and H. Linnartz, *Astronomy & Astrophysics*, 2009, **504**, 891-913.
46. H. Schneider, A. Caldwell-Overdier, S. C. t. Wallant, J. Huang, L. Dau, I. Nwolah, M. Kasule, C. Buffo, E. Mullikin, A. Hay, S. T. Bao, J. Perea, M. Thompson, M. V. Tuyl, A. Wang, S. Bussey, N. Sachdev, C. Zhang, M. C. Boyer and C. R. Arumainayagam, *Mon. Not. R. Astron. Soc. (accepted)*, 2018.
47. M. Bertin, C. Romanzin, M. Doronin, L. Philippe, P. Jeseck, N. Ligterink, H. Linnartz, X. Michaut and J. H. Fillion, *Astrophys J Lett*, 2016, **817**, 6.
48. B. McGuire, C. Shingledecker, E. Willis, A. Burkhardt, S. El-Abd, R. Motiyenko, C. Brogan, T. Hunter, L. Margules, J. Guillemin, R. Garrod, E. Herbst and A. Remijan, *Astrophys J Lett*, 2017, **851**, L46.

49. E. Mullikin, P. van Mulbregt, J. Perea, M. Kasule, J. Huang, C. Buffo, J. Campbell, L. Gates, H. M. Cumberbatch, Z. Peeler, H. Schneider, J. Lukens, S. T. Bao, R. Tano-Menka, S. Baniya, K. Cui, M. Thompson, A. Hay, L. Widdup, A. Caldwell-Overdier, J. Huang, M. C. Boyer, M. Rajappan, G. Echebiri and C. R. Arumainayagam, *ACS Earth and Space Chemistry*, 2018, **2**, 863.
50. M. Forstel, Y. A. Tsegaw, P. Maksyutenko, A. M. Mebel, W. Sander and R. I. Kaiser, *Chemphyschem*, 2016, **17**, 2726-2735.
51. T. I. Hasegawa and E. Herbst, *Mon Not R Astron Soc*, 1993, **263**, 589-606.
52. R. T. Garrod, *Astrophysical Journal*, 2013, **765**, 29.
53. C. N. Shingledecker, J. Tennis, R. Le Gal and E. Herbst, *Astrophysical Journal*, 2018, **861**, 15.
54. C. N. Shingledecker, R. Le Gal and E. Herbst, *Physical Chemistry Chemical Physics*, 2017, **19**, 11043-11056.

### **Key Learning Points**

1. Photochemistry and radiation chemistry of interstellar ices near star-forming regions lead to the extraterrestrial synthesis of prebiotic molecules
2. Photochemistry comprises chemical processes initiated by photon-induced electronic excitation not involving ionization.
3. In contrast, radiation chemistry involves both electronic excitation and ionization.
4. Radiation chemistry is mediated by low-energy electrons which may have reaction cross sections several orders of magnitude larger than those of photons.
5. Because the ionization threshold is lower in the condensed phase than in the gas phase, most “photochemistry” studies of astrochemistry likely involve radiation chemistry.